UNIVERSITAT POLITÈCNICA DE VALÈNCIA

ESCUELA TÉCNICA SUPERIOR INGENIERÍA INDUSTRIAL VALENCIA

INDUSTRIAL ENGINEERING MASTER THESIS

ANALYSIS AND DESIGN OF CU2O/ZNO OPTOELECTRONIC THIN LAYERS BY ELECTRODEPOSITION

AUTHOR: CORENTIN DENET

SUPERVISOR: DAVID JERONIMO BUSQUETS MATAIX

Academic year: 2020-21

Analysis and design of Cu_2O/ZnO optoelectronic thin layers by electrodeposition

Acknowledgements

First and foremost, the year 2020 has been for everybody one of the most unexpected year. Both academically, professionally, socially, and mostly personally. The sanitary crisis has had a considerably impact of everyone's mind. The human being had to adapt itself for this new way of life, which is, sadly, still going on in 2021.

I must admit that my master thesis for my ninth semester in Valencia was the roughest morally speaking. Even though I discovered a fabulous new way of life, met brilliant new people and experienced astonishing landscapes, I never had the chance to go to the laboratory even once, while I was seeing most of my schoolmates going. The Covid-19 virus prevented me to experience how is the real life of a researcher. This is, thus, my biggest disappointment. I really mean it. Indeed, I was waiting a lot from this internship, because I was still unsure about what to do after my engineering school, and a PhD was one of my top wishes before. Now I am rather scared not to be made for this kind of career.

Anyway, I know it has been particularly difficult for all. That is why, secondly, I really would like to thank first my mentor: David Jeronimo Busquets Mataix. Even if I never met him in person, he always responded present to answer my questions and to reassure me because of my non laboratory results. We both would have wished another unfolding.

The very same with my school in Nancy, France: Ecole Européene d'Igénieurs en Génie des Matériaux (EEIGM). In one hand because they gave me the opportunity to travel and discover new ways of life, both in Sweden and in Spain. I feel more than grateful about it. In another hand because mostly Valérie Vitzthum and David Horwat were there to support me during my uncertainties.

A special thanks to my parents as well, who helped me to undergo and to outdo this situation.

Afterwards, even if did not go as I had imagined, it will stay in my mind as a good experience and now I am looking forwards to new adventures and challenges.

Thank you again.

Abstract

During this study, a solar cell was designed. A chemically electrodeposited zinc oxide and copper oxide heterojunction cell was designed.

Indeed, such a cell was found to have excellent and promising optical and electrical properties, due to their natural p-type and n-type and their highly exploitable band gap as a semiconductor.

This work thus presented the different deposition factors that influence the structure and morphology of the layers present in the device as well as their electrical and optical properties. However, before that a state of the art was written. It presents the solar cells and how they work by explaining in depth the p-n junction. Then the characteristics of the two oxides concerned were highlighted as well as the manufacturing and characterization techniques such as x-ray diffraction or J-V measurement.

It was therefore stressed that the important factors to be controlled during deposition were the pH of the bath, the deposition temperature, the applied current and of course the thickness of the thin oxide layer. All these parameters were listed and studied according to the different characterization techniques. The influence was noticeable mainly on the preferential growth structure of both semi-conductors. Indeed, the wurtzite crystalline structure of ZnO displayed a favourable (002) orientation due to its epitaxially behaviour with ITO substrate and Cu_2O. The same thing appeared with copper oxide with a preferential (111) direction growth where it shows their best properties as solar cell.

Key words: thin film solar cell, Cu_2O, ZnO, p-n junction, electrochemical deposition

Resumen

Durante este estudio, se diseñó una célula solar. Se diseñó una célula de heterojunction de óxido de zinc y óxido de cobre electrodepositado químicamente.

De hecho, se descubrió que dicha célula tenía excelentes y prometedoras propiedades ópticas y eléctricas, debido a su tipo p natural y su tipo n y a su gran aprovechamiento del hueco de la banda como semiconductor.

Así pues, en este trabajo se presentaron los diferentes factores de deposición que influyen en la estructura y morfología de las capas presentes en el dispositivo, así como sus propiedades eléctricas y ópticas. Sin embargo, antes de eso se escribió un estado del arte. Presenta las células solares y cómo funcionan explicando en profundidad la unión p-n. A continuación se destacan las características de los dos óxidos en cuestión, así como las técnicas de fabricación y caracterización como la difracción de rayos X o la medición J-V.

Se subrayó, pues, que los factores importantes que debían controlarse durante la deposición eran el pH del baño, la temperatura de deposición, la corriente aplicada y, por supuesto, el espesor de la fina capa de óxido. Todos estos parámetros se enumeraron y estudiaron de acuerdo con las diferentes técnicas de caracterización. La influencia fue notable principalmente en la estructura de crecimiento preferencial de ambos semiconductores. De hecho, la estructura cristalina de wurtzita del ZnO mostró una orientación favorable (002) debido a su comportamiento epitaxial con el sustrato ITO y el Cu2O. Lo mismo ocurrió con el óxido de cobre con un crecimiento de dirección preferencial (111) donde muestra sus mejores propiedades como célula solar.

Palabras clave : célula solar de película fina, Cu2O, ZnO, unión p-n, deposición electroquímica

Resum

Durant este estudi, es va dissenyar una cèl·lula solar. Es va dissenyar una cèl·lula d'heterojunction d'òxid de zinc i òxid de coure electrodepositado químicament.

De fet, es va descobrir que la dita cèl·lula tenia excel·lents i prometedores propietats òptiques i elèctriques, a causa del seu tipus p natural i el seu tipus n i al seu gran aprofitament del buit de la banda com a semiconductor.

Així, doncs, en este treball es van presentar els diferents factors de deposició que influïxen en l'estructura i morfologia de les capes presents en el dispositiu, així com les seues propietats elèctriques i òptiques. No obstant això, abans d'això es va escriure un estat de l'art. Presenta les cèl·lules solars i com funcionen explicant en profunditat la unió p-n. A continuació es destaquen les característiques dels dos òxids en qüestió, així com les tècniques de fabricació i caracterització com la difracció de rajos X o el mesurament J-V.

Es va subratllar, perquè, que els factors importants que havien de controlar-se durant la deposició eren el pH del bany, la temperatura de deposició, el corrent aplicada i, per descomptat, la grossària de la fina capa d'òxid. Tots estos paràmetres es van enumerar i van estudiar d'acord amb les diferents tècniques de caracterització. La influència va ser notable principalment en l'estructura de creixement preferencial d'ambdós semiconductors. De fet, l'estructura cristal·lina de wurtzita del ZnO va mostrar una orientació favorable (002) a causa del seu comportament epitaxial amb el substrat ITO i el Cu2O. El mateix va ocórrer amb l'òxid de coure amb un creixement de direcció preferencial (111) on mostra les seues millors propietats com a cèl·lula solar.

Paraules clau : cèl·lula solar de pel·lícula fina, Cu2O, ZnO, unió p-n, deposició electroquímica

Table of contents

Index of illustrations

Index of tables

1. Introduction

Motivation

Nowadays, the need for energy is increasing in a world where the industrialized countries, which are constantly making energy-intensive technological progress, and in a world faced to an expected world population at 2.5 billion in 1950. This significant demographic growth will certainly be accompanied by an increase in energy consumption, particularly of fossil fuels such as oil, gas, and coal, which constitute the main source of energy production, especially electrical energy. Nevertheless, fossil reserves are limited and will be exhausted within a few decades. Moreover, the consumption of fossil fuels leads to air pollution and pollution of the atmosphere. production of greenhouse gases such as carbon dioxide, nitrogen oxides and greenhouse gases. Halogenated hydrocarbons which are the cause of a worrying global warming. The need to address these problems results in the design and study of many renewable energies. Among them, solar energy has proved to be promising in the production of photovoltaic energy (Koussi-Daoud, 2016a)

Justification

Photovoltaic energy, which consists of the conversion of light energy into electrical energy, has therefore undergone a notable development with the appearance of different generations of cells (Koussi-Daoud, 2016a). Photovoltaic energy knows a production of 47% (Ananda, 2017) per years which justify the fact this energy attracted the attention of the world and could be a tremendous advance for the innovation and the ecology. Even though it does exist several solar cells now, one is considerably starting to be considered. ZnO/Cu_2O heterojunction solar cell is indeed a low-cost, non-toxic for the human being and abundant in out planet earth. Moreover, recently a high conversion efficiency regarding this solar cell has been achieved: around 4% (*Fabrication and Characterization of Copper Oxide-Zinc Oxide Solar Cells Prepared by Electrodeposition - IOPscience*, n.d.), which is more than considerable for this device (Minami et al., 2011). However,r this was deposited by thermal oxidation which is excellent but expensive. That is why a low-cost electochimical deposition will be preferred. Furthermore, both ZnO and Cu_2O semiconductor show a natural n-type and p-type behaviour, respectively. Copper oxide has a direct band gap of around 2 eV (Tran et al., 2018) and ZnO a direct wide band gap of 3,3 eV (Yeul & Dhote, n.d.). 20% (Tran et al., 2018) is the theorical power conversion efficiency of an cuprous oxide.

Objective

The aim is thus to investigate such a cell, they are very promising. However, the recorded PCE is still very low compared to the already commercialized solar cells. In this project different electrodeposition parameters will be scrutinized in order to exhibit how is the device influenced by them, to chose the best among them and to design such solar cell.

2. A state of the art

In this section, a state of the art of the entire work will be carried out. The aim is to have a better understanding of what already exists concerning solar cells and more particularly how Cu_2O/ZnO thin film solar cells (TFSCs) are fused. How they are characterized and how it could be outlooked in the future.

2.1. Solar cells

First and foremost, a solar cell is a device which is constantly coveted by the researchers over the past decade. Indeed, it converts natural energy, well-known as sun lights, into electricity (Işık, 2015). Nowadays it is more than necessary to find a sustainable and an eco-friendly way to produce electricity. This is called photovoltaic energy conversion. This energy could permit to avoid the use of fossil fuels which are damaging and more and more scarce (Hamakawa, 2013). However, creating an electric current thanks to the cell is a long process and moreover, there is numerous materials and types which could suit solar cells as refer *Figure 1*.

Usually p-n junction (Gibbons, 1977) semiconductor materials are used in this field in order to reach high power conversion efficiency (PCE). This section will, thus be dedicated to the five different types of solar cells the most used nowadays before giving information of what a semiconductor is and how a p-n junction does work.

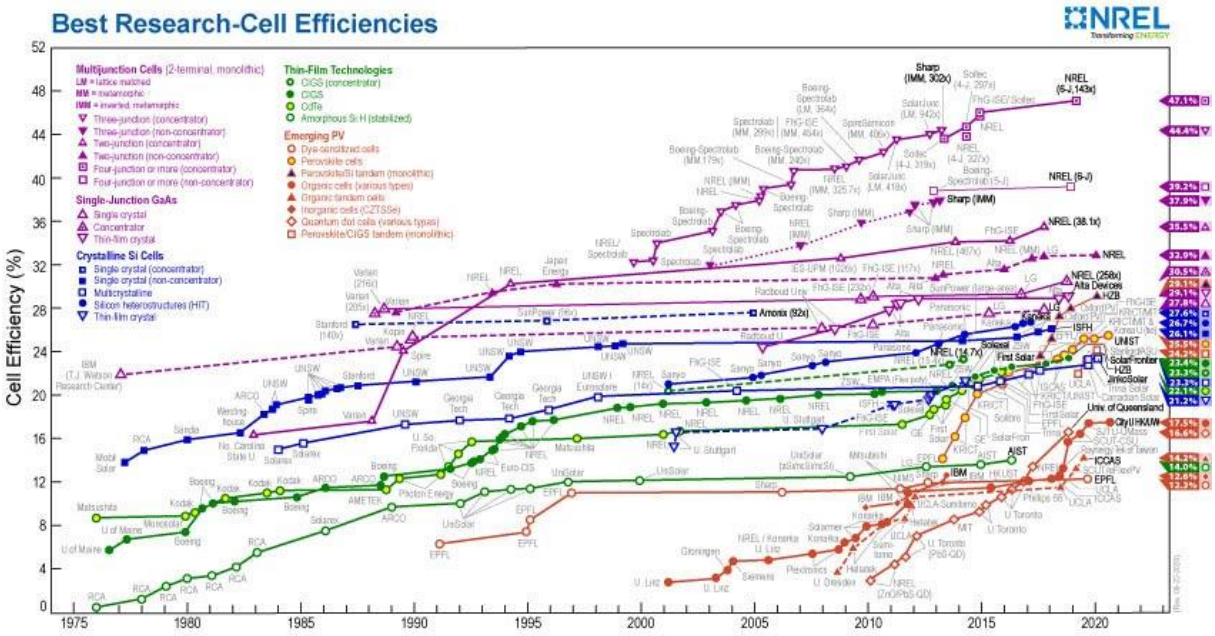

Figure 1: Efficiency of different solar cells through the years (NREL, 2019)

2.1.1. Multijunction solar cells (MJSCs)

A multi-junction cell is a cell consisting of several semiconductors assembled with each other. Commonly known as a tandem cell, they have the advantage of being able to combine the efficiency of the best semiconductors, which proves to be very useful.

As an example, the most manufactured multijunction cell is the lattice matched (LM) GaInP/GaInAs/Ge, as viewable in *Figure 2*.

It is known to have reached a PCE of 44% (*McEvoy's Handbook of Photovoltaics*, 2018) with a rather long lifespan. However, the assembled semiconductors must be carefully chosen, as they must have a very similar or even identical crystal structure. Therefore, this type of cell is always a challenge.

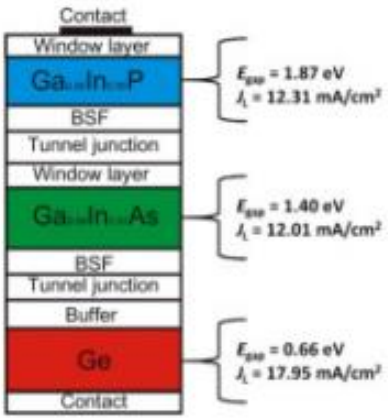

*Figure 2: Scheme of a typical LM (*McEvoy's Handbook of Photovoltaics, *2018)*

2.1.2. Monocrystalline silicon solar cells (MSSCs)

Today MSSCs are one of the most used solar cells if not the number one. The word "mono" is used to refer to the fact that solar cells are made of a singular silicon crystal. The crystallographic structure of silicon is represented *Figure 3*. Pure silicon is molten at high temperature after which a crystal seed is added. The molten silicon forms afterwards all around the seed which corresponds to the single crystal. They are the cut into little pieces. In a general way, 60 MSSCs composed a whole solar panel. Compare to either polycrystalline silicon solar cells (PSSCS) or TFSCs, MSSCs display the best PCE so far. These commercially available solar panels have an efficiency ranging from 17% to 22% (*Types of Solar Panels*, n.d.). Obviously, since this a monocrystalline cell, electrons are enabled to circulate easier inside the cell, which is considerable regarding the efficiency of the device.

Although they are the most commercialized, the main issue for this kind of solar panel is the cost (Kalogirou, 2009). Their high efficiency and the manufacture have driven up the price. This has therefore become a significant disadvantage, hence the need to study and develop other viable systems as this project is dedicated. This structure, as shown in *Figure 3* (Said-Bacar, n.d.), makes the cells as well as the panel black.

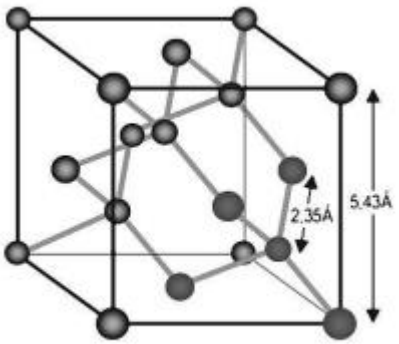

Figure 3: Crystallographic structure of a monocrystalline silicon

2.1.3. Polycrystalline silicon solar cells (PSSCs)

It is well-known that PSSCs are less efficient that MSSCs (Kalogirou, 2009). They are created similarly the same way of MSSCs. Nevertheless, the seed crystal is extracted once silicon is cooled down. This cooling process ends up with the formation of multiple crystals. Having a multi-crystal structure will make the movement and circulation of electrons much harder and less fluid than within a single crystal. As a matter of fact, the disorder induced by the grain boundaries and the distortion of the bonds between the silicon atoms cause a distribution of electronic states (Said-Bacar, n.d.). Their efficiency is nonetheless honourable knowing that it is around 15% and 17% (*Types of Solar Panels*, n.d.). This device is still on improvement as every kind of solar cells.

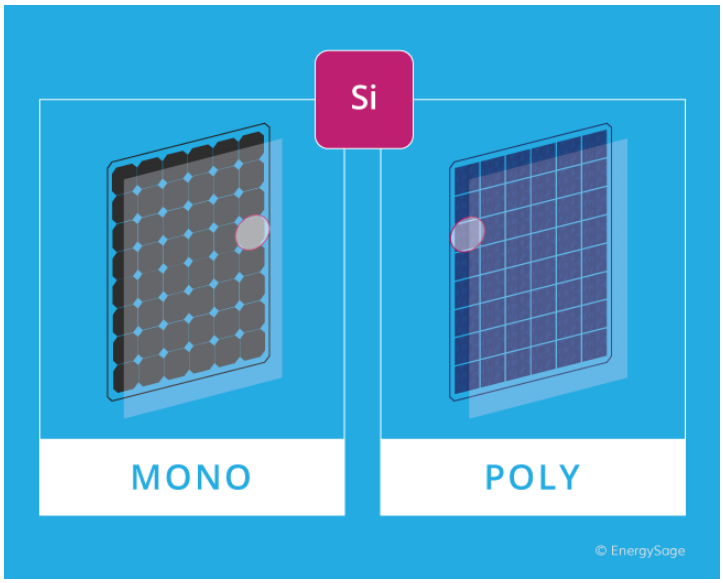

Figure 4: A monocrystalline and a polycrystalline solar panel

Due to the fact that, these cells have a lower manufacturing cost and efficiency than MSSCs, these panels have become a very interesting understanding for people who want to install solar panels at homes. This kind of solar panels, as noticeable in *Figure 4* (*Types of Solar Panels: What Are Your Options? | EnergySage*, n.d.) are bluer.

2.1.4. Perovskite solar cells (PSCs)

Over the past decade, PSCs based on hybrid organic-inorganic metal halide perovskite absorber layers, which has its crystallographic structure shown *Figure 5* (Eames et al., 2015), have come up as one of the most promising emerging photovoltaic technologies, increasing from 3.8% of efficiency in 2009 (Kojima et al., 2009), to 25.2% in 2020 – for single-junction architectures – and 29.1% in silicone-based tandem cells (NREL, 2019), exceeding the maximum efficiency achieved in single-junction silicon solar cells and narrowing the gap with the Shockley-Queisser theoretical limit of 33.7% for a single p-n junction (Shockley & Queisser, 1961). Moreover, these materials can be prepared from solution-based methods and yet display optoelectronic features equivalent to older, classic solid-state semiconductors. This has resulted in photovoltaic devices that can be prepared at ambient temperatures, and still attain power conversion efficiency (PCE) levels comparable to already-widespread polycrystalline silicon (NREL, 2019). Despite the fact that their fundamental working principles are not yet fully established – therefore remaining a subject matter for research, PSCs can be viewed as the currently fastest-advancing solar technology, presenting a growing commercial interest thanks to their very low-cost production and ever higher potential efficiencies.

But a considerable issue remains, as PSCs are not stable enough in the long-term when submitted to temperature variations (Schwenzer et al., 2018), moisture (Leguy et al., 2015), oxygen (Aristidou et al., 2017), UV radiation (Farooq et al., 2018) and elevated temperatures (Bastos et al., 2019; Domanski et al., 2018). In order to be competitive, PSCs must warranty a minimal power output of 80.2% of the initial power output after 15 years, which is a common value for other conventional photovoltaic technologies such as Si and GaAs solar cells (*Canadian-Solar-Warranty-12-Years.Pdf*, n.d.). In terms of real-life application thermal degradation, which is now one of the main issues to be addressed, they should also be able to withstand temperature rates of up to 100 °C/h and temperatures up to 85 °C (*IEC 61646 - Thin-Film Terrestrial Photovoltaic (PV) Modules – Design Qualification and Type Approval | Engineering360*, n.d.)

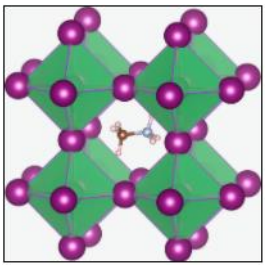

Figure 5: Typical structure of methylammonium lead halide; the $CH_3NH_3^+$ cation is surrounded by corner-sharing PbX_6 octahedra

2.1.5. Thin film solar cells (TFSCs)

A thin-film solar, which is considered to be the new generation of solar cells cell (Işık, 2015), is generally composed of several thin layers of semiconductor materials as well as a substrate (Lee & Ebong, 2017). It does exist numerous types of thin-film device, as exposed in *Figure 6*, which have their own shaping process. They can be up to 300 times thinner than the devices shown above (*What Are Thin Film Solar Panels, How Do They Work and Why Aren't They Used for Residential Solar Systems?*, n.d.). As a result, this implies a considerable reduction, firstly, in the weight and, secondly, in the cost of the solar cell.

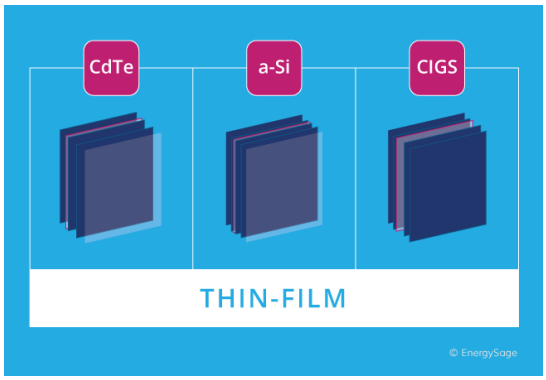

*Figure 6: A thin-film solar panel (*Types of Solar Panels: What Are Your Options? | EnergySage*, n.d.)*

However, this type of device may contain certain substrates that are toxic to humans and the environment. Moreover, its efficiency is lower compared to other systems, with a PCE of between 4% and 12% (*Types of Solar Panels*, n.d.). This is indeed what will catch the eye of researchers. Thin-film solar cells, due to their low cost, have many areas for improvement. Indeed, this project will focus on the study of thin-layers Cu_2O/ZnO production.

2.1.6. Semiconductors

Materials could be divided into three categories: conductors, insulators and, in between, semiconductors (*Figure 7*). As the name suggests, these materials are known to have electrical resistivity between insulators (>10^{+6} Ω.cm) and metals (<10^{-4} Ω.cm) (Helaili, n.d.). Its main characteristic is to have a filled valence band and a conduction band ready to accept electrons. In fact, between these two bands is the band gap also called energy gap (Eg). Its value for these materials must be between 0.1 and 3.2 eV precisely. In other words, below this value the material will basically be a metal (conductor) and above that an insulator. The value of 3.2 eV has been calculated theoretically. The maximum energy provided by the visible spectrum corresponds to the wavelength of violet, i.e., about λ = 400 nm. To produce a photon, the following relationship is given:

$$\boldsymbol{E = h \times v}$$ with h = 6.63 x 10^{-34} $m^2.kg.s^{-1}$ Planck's constant

Moreover, knowing that the frequency of radiation v is calculated in this way:

$\boldsymbol{v = c \div \lambda}$ with **c** = 3 x 10^8 m.s^{-1} light velocity

This energy obtains in joules may be easily converted in eV (1 eV = 1,6.10^{-19} J) this falls on the value given previously,3.2 eV (Chawake, 2014).

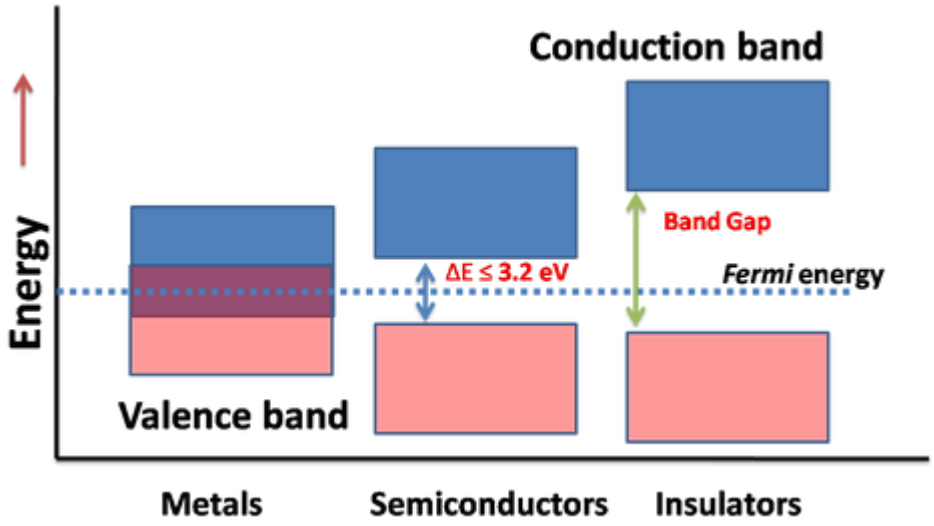

Figure 7: Energy bands comparison between conductors, semiconductors and insulators materials (Chawake, 2014)

If an energy source provides enough energy to the semiconductor, an electron is excited and goes from the valence band up to the conduction band and leaves behind a hole. It, hence, is going to create electron-hole pairs inside the device. This is what will be at the origin of conductivity. The conductivity will then depend on several factors, namely, the illumination provided by the sun in this case, the temperature, and the presence of impurities in the material known as doping (intentional or unintentional). This will be discussed in detail in the next section, but doping increases the charge carrier density within the material. Therefore, it will change the type of conduction and transport properties.

2.1.7. A p-n junction solar cell

For information purpose, p-n junctions are found in a multitude of electronic devices such as diodes and it is on this same junction that solar cells are based. Fundamentally p-n junction is obtained by combining one material who has a majority of electrons carrier with another who has a majority of holes carrier. This means respectively a n-type and a p-type material. For the most known and used solar cells, such as monocrystalline/polycrystalline silicon or perovskite, it is a necessity to dop the cell. In other words, it is mandatory to integrate impurities into them. On the contrary, this will be seen later, semiconductors such as Cu_2O and ZnO are investigated to be natural p-type and n-type respectively. In other words, it does exist two types of semi-conductors:

- **Unintentional doping**: as highlighted above, Cu_2O and ZnO are extremely well known to be p- and n-type semiconductors respectively, naturally. That is to say that the material intrinsically

has uncontrolled defects in the crystallographic structure (gaps, excess of atoms or impurities). For instance, Cu_2O displays a lack of copper atoms and in order to keep the electronic stability of the device certain atoms of copper are found in the Cu^{2+} form instead of Cu^{+}, this result, hence, in a lack of electrons in the valence band: a p-type doping is obtained. Same thing happens concerning ZnO. This is therefore very advantageous in the field of energy conversion. Indeed, the hole and electron density will increase. This will become highly exploitable regarding solar cells. This unintentional doping depends a lot of the fabrication process. Therefore, it might be an avenue to be explored in order to improve the performance of the Cu_2O/ZnO solar cell (Bergerot, n.d.).

- **Intentional doping:** basically, the case of silicon, which is today the most commercially available solar cell. It is found in both monocrystalline and polycrystalline forms. The monocrystalline form is more efficient in terms of converting solar energy into electrical energy but is much more expensive as explained above. One of the reasons it is more expensive is that it needs to be chemically doped. It consists of voluntarily introducing one or more other atoms into the material, chosen according to their electronic structure. For example, silicon has 4 valence electrons on its outer layer. In order to obtain an n-type junction for silicon, it is known to incorporate phosphorus instead of certain silicon atoms. Indeed, since phosphorus has 5 valence electrons, it will then create a free electron that is easy to excite. Thus, creating a large quantity of negative charge carriers. This is how n-type doping is carried out. Conversely, boron has only 3 electrons in its outer layer, so by substituting it for silicon, it will be able to bond with 4 silicon atoms, but one of the 4 bonds will only be made with a single electron. One electron will therefore be missing in relation to silicon, which means that a hole has been introduced. This gap can be filled by an electron from another bond, but this other bond will then present a gap in turn: the gap has moved, which is equivalent to say that the hole has moved. The introduction of boron therefore introduced a moving hole in the material and therefore a p-type doping (Bergerot, n.d.).

Considering, then a p-type copper(I) oxide and a n-type zinc oxide solar cell device which are two different materials, during their assembly it is in this case a question of heterostructures or heterojunction (Abd-Ellah et al., 2016; Benhaliliba et al., 2017).At this point, if the junction between p-type and n-type materials is made, the device will immediately start to work. Indeed, the device will try to attain the equilibrium. As long as, there is an excess of electrons in the n-type junction and of holes in the p-type area, they are going to, trough the junction, combine themselves. Which is representing a numerous motion of charges. That means, afterwards that the negative charges of the n-type side will go in the p-type side. Resulting with a drop of electron concentration in the n-side and an increase in the p-side and ending up with a difference of polarity and thus the emergence of an electric field which goes from the n-type to the p-type. This field is the consequence of the creation of layer composed only of static charges called the depletion layer. The direction of the electric field is important, that means that electrons will try to go on the opposite direction. Leading to the formation of a layer nearby the junction of static negatively charge carriers in the p-area and static positively charge carriers in the n-side. The layer is called as the depletion layer (Shahrestani, 2013).

Each semiconductor material has their own electrical properties (valence band, conduction band, band gap, carrier lifetime ect…) (HITACHI, n.d.). Photons produce by the sun rays are absorbed by the cell. These photons need to have a certain energy to excite an electron to let it reach the conduction band of the material. If it is the case electrons will be removed nearby the p-n junction leading to the

formation of holes. Naturally, holes will be filled by the contribution of electrons which will circulate in the crystalline network in the p-side. The electrons released by the sufficient energy of the photon to shift the charge from the valence band to the conduction band will move to the n-zone where there is an excess of positive charge. Due to the magnetic field created by the p-n junction, electrons and holes will not be able to recombine for some time. This means that an accumulation of opposite signs will occur, so if we connect n and p externally then the electrons will be able to circulate and create an electric current. A schematic representation of a p-n junction at thermal equilibrium in *Figure 8* is displayed.

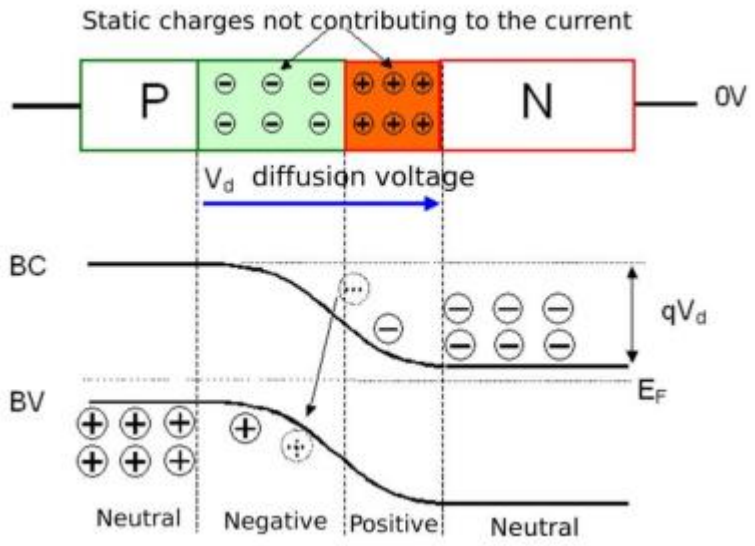

Figure 8: Zero bias applied p-n junction (Shahrestani, 2013)

The open circuit voltage is a concept extremely important for a solar cell. The light generated carriers are conducted towards contact terminal which create, thus a different voltage of both side of the device. More the drop of the voltage is wide more the open circuit voltage is efficient and better will be the light conversion into electricity of the photovoltaic cell. Usually The external quantum efficiency (EQE) of a cell is determined by the number of photons converted into light carriers within the cell. Generally, it depends on the chosen semiconductor and particularly on the value of its band gap. In fact, thanks to this, a material will be more suitable for energy conversion at certain wavelengths. The EQE also depends on the probability of charge recombination. A short carrier distance will be preferred due to a lower probability of recombination (T. Wang et al., 2019). And this of course depends on the intrinsic properties of the selected semiconductors.

2.2. Copper(I) oxide semiconductor

Before being a semiconductor nanomaterial for solar cell devices, copper oxide is more commonly found in the form of bulk materials. It is a mineral that can easily be found in nature under the name

of cuprite. It is a red coloured (*Figure 9*) compound whose formula is Cu_2O. Normally it is widely used as a pigment for glass and ceramics.

Most interesting for this study is the fact that copper oxide has natural p-type semiconducting properties known since the 1917s and ever since but more recently, it has been deeply studied as a future material for solar cells (Olsen et al., 1982). The very first known oxide with semiconducting properties. It was even used as a semiconductor long before silica, which appeared in the 1940s (Bergerot, n.d.).

*Figure 9: Cuprite powder (*Cuprous Oxide | Metal-Powder-Dust.Com*, n.d.)*

2.2.1. General properties

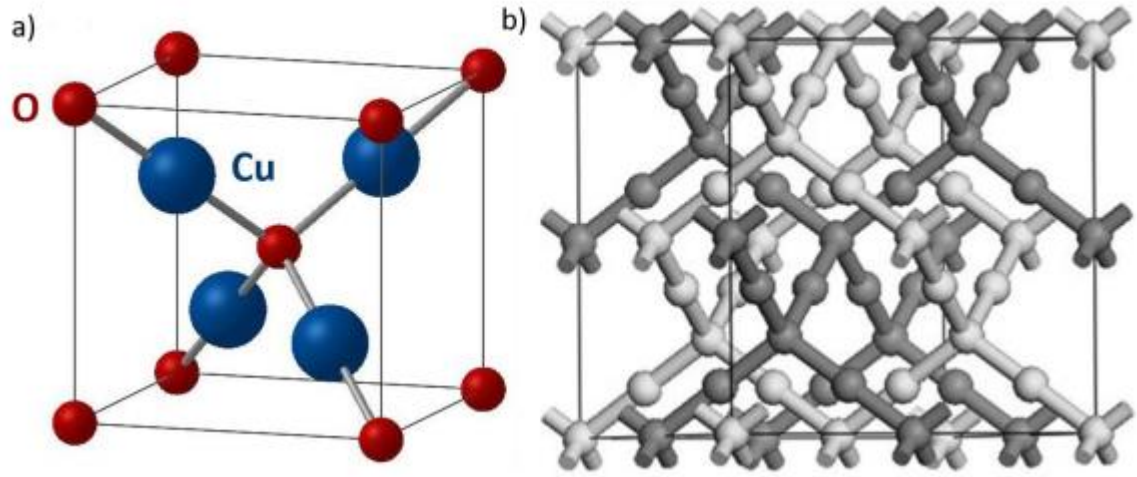

Figure 10: a) Cu_2O crystallographic structure. (b) 2x2x2 atomic structure cells of Cu_2O (Resende, 2017)

Nowadays this semiconductor has many advantages among others such as silicon or even better the perovskite known as calcium titanium. Indeed, this ore is present in nature in abundant quantities, it

is not expensive and not toxic (Bergerot, n.d.; Koussi-Daoud, 2016b; Resende, 2017; Salek, 2013; Shahrestani, 2013). Its crystalline structure (*Figure 10*) is cubic with oxygen atoms arranged in a centred cubic (CC) structure and copper atoms occupy the centre of half of the a/2 edge cubes (Salek, 2013). The mesh parameter a = 4.2696 Å. This structure has the properties, in stoichiometric condition, a density of 6.10 $g.cm^{-3}$ and a molar mass of 143.09 $g.mol^{-1}$ (Resende, 2017).

Copper oxide is known, as a semiconductor, to have a wide band gap of the order of 2eV and a high absorption coefficient. This value is likely to be different according to the articles. The most accurate value to propose is 2.137 eV. In other words, this means that it partially or totally absorbs light from wavelengths below 580 nm (blue range) and therefore transmits light at higher wavelengths (yellow and green range). Therefore, Cu_2O appears yellow and transparent to the naked eye, making it a significant candidate for the formation of transistors and photovoltaic cells (Bergerot, n.d.). Basics properties of Cu_2O are set forth in *Table 1*.

Table 1: Basics properties of Cu_2O (Olsen et al., 1982)

Band gap	~2.0 eV
Electron affinity	3.2 eV
Crystal structure	Simple cubic
Lattice constant	4.2696 Å
Melting point	1235°C
Density	6.0 $g.cm^{-3}$
Thermal expansion coefficient	3.5 x 10^{-6} $°C^{-1}$
Conductivity type	p type

Thanks to *Figure 11* that displays the number of publications about Cu_2O semiconductors through the years. Irrefutably it currently grows tremendously. The needs of finding the right material for green solar cells device in order to answer the question of the environmental and the human being protection is, sadly, hurrying up.

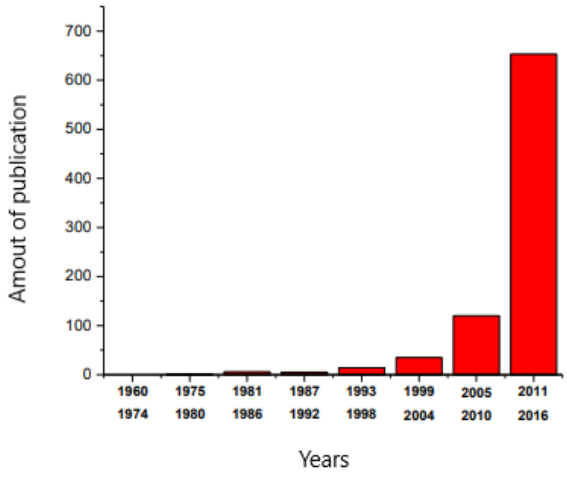

Figure 11: Estimated numbers of publication about Cu_2O semiconductor solar cells during the years (Koussi-Daoud, 2016b)

2.2.2. Electric conduction

Many defects are present within the copper oxide structure. These defects can be explained by the presence of excess oxygen leading to the formation of copper atom lacunae . As shown in *Figure 12* the 2p levels of oxygen, which has a high electronegativity, will create a strong valence band edge. This results in a low mobility of the holes in relation to its effective mass. However, the $3d^{10}$ levels of Cu^+ will form the top of the valence band and therefore improve the mobility of the holes (Resende, 2017). This explains its p-type electrical conductivity This gives it a wide mobility of positive carriers at room temperature, μ_p~100 $cm^2.V^{-1}.s^{-1}$, from the moment it is manufactured in a thin layer.

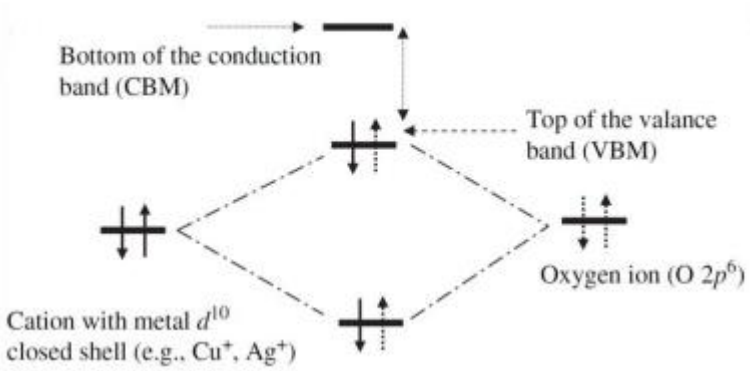

Figure 12: Chemical bond between an oxide ion and a cation with closed metal d shell (Resende, 2017)

Elaboration will have to play a major role concerning the structure of the copper oxide and will then have an impact on its properties. Indeed; there is certain parameters regarding the creation of Cu_2O semiconductor which have to be carefully under controlled, always in order to enhance the efficiency (Salek, 2013) of Cu_2O as a solar cell.

2.2.3. Cu_2O for solar cells

Currently, it is without doubts that copper oxide is one of the main candidates regarding solar cells application. As specified before, Cu_2O shows up a natural p-type behaviour. This is explained by the formation of Cu vacancies in the crystal structure (Nolan & Elliott, 2006). As a matter of fact, 20% is the maximum power conversion efficiency concerning Cu_2O which has been theoretically calculated, taking into account that current losses are only causing by the injection of minority carriers within the junction. Investigations reported to expect, in a viable way, efficiencies up to 9% (Olsen et al., 1982). Nowadays the highest PCE achieved by Cu_2O, included as an active layer in MgF_2/Al-doped ZnO/$Zn_{0.38}Ge_{0.62}$-O/Cu_2O, is knowing to be 8,1% (Jayathilaka et al., 2020) . All of this proves considerably the strength of this semiconductor.

Nevertheless, compare to the other devices already commercialized, copper oxide-based solar cells need obviously enhancements and thus further research. These researches have to be oriented on

three mains issues that Cu_2O solar cells are exposed to, namely junction formation, material growth direction and photocurrent.

2.3. Zinc oxide semiconductor

The use of zinc oxide, a white (*Figure 13*) inorganic compound (when it is pure) (Yeul & Dhote, n.d.), as a promising compound in the field of light-emitting diodes or solar cells semiconductors (Hamid, 2009) in particular was discovered at a late stage. Indeed, even before the 2000s, the main applications of ZnO were dedicated to the pharmaceutical and chemical industries (Hadouchi, 2017). It is also well known to be used as an additive in numerous materials such as rubber (~36%) (Karam, 2017).

It was in 1968, by Daprak (Karam, 2017), that the possibility of manufacturing light-emitting diodes (LEDs) was discovered. Currently, this element has become an actively coveted and studied material because of its more than interesting chemical and physical properties (wide band gap semiconductor, large exciton binding energy, low-cost synthesis, possibility of depositing different morphologies of nanostructures, etc.) in photovoltaic applications.

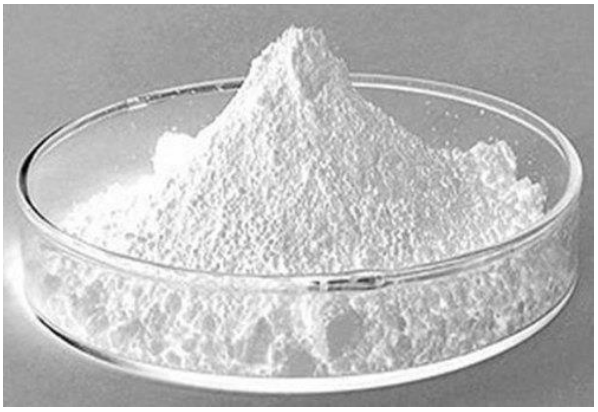

*Figure 13: 99,5% pure Zno powder(*Zinc Oxide Nanoparticles*, n.d.)*

2.3.1. General properties

Just like copper oxide, ZnO attracts the attention of researchers because this element is inexpensive, abundant in nature and non-toxic (Hadouchi, 2017; Karam, 2017; Luo, 2020; Yeul & Dhote, n.d.). Here are the main characteristics that are increasingly sought after in the construction of solar panels.

Naturally, this oxide is called zincite. Three different crystal structures of ZnO are known, the hexagonal type, the würtzite form, zinc blende or rocksalt. However, as it can be seen in *Figure. 14*, without any change in structure, the latter can be found in the thermodynamically stable form of würtzite, belonging to space group $P6_3mc$ (Hadouchi, 2017), under normal pressure and temperature conditions. This structure therefore corresponds to a stack of compact double layers along the c (0001) axis formed, obviously, by oxygen and zinc atoms with the following lattice parameters: a = 0.32495

nm and c = 0.52069 nm. The ratio c/a = 1.602 is visibly very close to the ideal compact hexagonal structure, i.e. c/a = 1.633 nm.

It is known that the achievement of one-dimensional ZnO nanostructures is greatly favoured by the anisotropic growth along the c-axis. This is due to the fact that the würtzite structure has no centre of symmetry and that the individual stacked planes lead to a dipolar moment between (0001) and (000-1) (spontaneous intrinsic polarisation). And since the surface energy in the (0001) plane is higher than in the other planes, this results in a higher growth rate along the c axis (Karam, 2017).

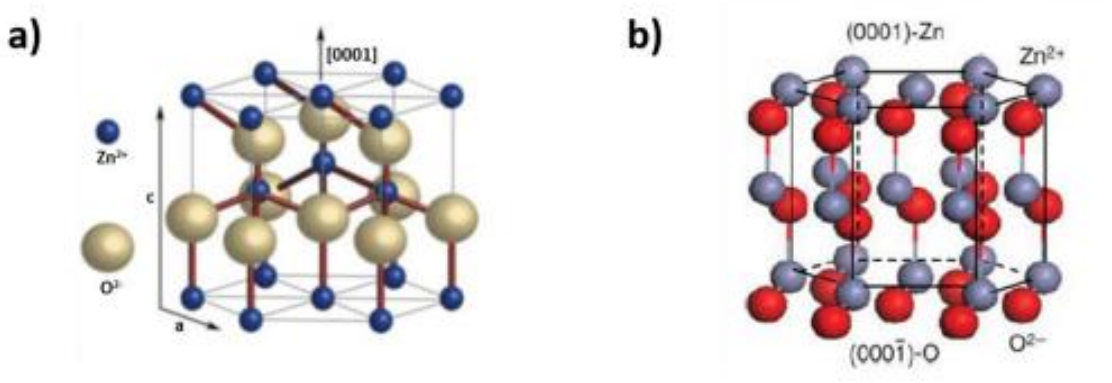

Figure 14: Crystalline structure of ZnO (Würtzite) (Karam, 2017)

Prepared under so-called classical conditions, at 300K, ZnO is a wide band gap semiconductor. Its value is about 3.30 eV without doping. When doped, it can reach up to 3.90 eV, as display in *Table 2*. This is often compared to gallium nitride (3.50 eV). Furthermore, thanks to this characteristic, it is transparent to the solar spectrum in the visible range and can be considered for optoelectronic applications in the blue and UV range.

This oxide will be preferred to the use of GaN when its binding energy is learned from the free exciton. Namely 60 meV for ZnO against 25 meV for GaN. This energy, shown by an absorption peak, is therefore really close from the gap. This makes it, thus, very promising for optical devices.

Table 2: Basics properties of Zno

Band gap (300 K)	~3,30 eV
Exciton binding energy	60 meV
Crystal structure	Würtzite
Volume density (300 K)	5,675g.cm^{-3}
Lattice constants	a = 0,32495 nm c = 0,52069 nm
Electrons mobility	205 cm^2.V^{-1}.s^{-1}
Melting point	1974 °C
Conductivity type	n-type

3.3.2 Electric conduction

As previously mentioned, zinc oxide is intrinsically n-type doped. This can be explained by the fact that the crystallographic structure has many gaps due to the large difference in ionic radius between the Zn^{2+} cation (r = 0.60 Å) and the O^{2-} anion (r = 1.38 Å). It appears that about 55% of the volume of the crystal is composed of voids. This therefore induces insertions of zinc atoms or impurities, leading to a stoichiometric imbalance of the oxide and then to an excess of electrons, thus creating electron donor centres within the structure. This is what happens in fact, the ZnO structure very often presents oxygen gaps or an excess of zinc that can be observed in the interstitial sites.

Zinc oxide has an electron mobility which varies between 10^{-3} and 10^{-2} $ohm^{-1}.cm^{-1}$ considering the undoped ZnO. As explained, in most cases, ZnO is intrinsically doped which increases its conductivity by between 10^{1} and 10^{2} $ohm^{-1}.cm^{-1}$.

This value can become even higher when the oxide undergoes extrinsic doping. Indeed, like silica, it is possible to incorporate impurities into the crystal lattice of the semiconductor. This doping takes place either by substitution or in the interstices, in the same way as silica. There is a wide variety of elements that can potentially doped ZnO. Doping the lattice is, however, economically, and temporally more expensive.

3.3.3 ZnO for solar cells

In many respects, ZnO tends to be a substitute to GaN an TiO_2. Zinc oxide shows a low cost production and better optical properties (Ozgur et al., 2010). This is therefore, why this material is attracting attention. ZnO is considered as the next generation of solar cells caused to its wide band gap in order to harvest enough sufficiency from the solar spectrum and so reach better PCE (Zhou et al., 2017). For now, the issue regarding ZnO based solar cells is the required p-type doping, which is leading to recombinant traps due to the crystal defects and thus to poor efficiencies and short circuit currents. This is the reason why, this study is going to use ZnO within a heterojunction solar cell. Zinc oxide semiconductor is mainly used as window layer and transparent thin film transistor (TTFT) (S. Jeong, 2010).

What is more than interesting with zinc oxide is that it is possible to control the growth of the single crystal rather easily. Indeed, it is through the different deposition techniques that the growth of the crystal lattice can be controlled. And therefore, have a significant impact on the optoelectronic properties.

2.4. Fabrications techniques

The performance of a solar cell, whether thin-film or otherwise, is determined by key optical and electrical properties. These different properties are a consequence of the way the cells are manufactured. Indeed, there are many different process methods for the manufacture of these cells.

Depending on the method chosen, the efficiency of the cell will be modified. It is therefore necessary to compare them in order to get an idea of the methods used.

This section will therefore be a presentation on the different methods of manufacturing ZnO/Cu_2O solar cells, presenting their influence on the electrical and optical properties and the quality of the layer interfaces.

The following techniques will be presented below:

- Chemical Vapor Deposition (CVD)
- Thermal oxidation
- Electrochemical deposition (ECD) which is the method related to this study.

This part will also prove that the efficiency of the cell is also depending on the used fabrication parameters. All these parameters will be more highlighted and explained for the ECD in the third section.

2.4.1. Chemical Vapor Deposition (CVD)

It is known, in the semiconductor industry, CVD is attractive firstly because regarding optoelectronic devices, this method is able to create epitaxial ZnO films and secondly because it is useful for mass production. It is mainly used for creating semiconductor film due to its aptitude to manufacture high-purity semiconductor (Siddiqui et al., 2012). Since ZnO is growing faster in the c-axis due to its anisotropic growth and columnar morphology (S. Jeong, 2010). This method improves, thus, the surface and the heterojunction of the device.

CVD process basically consists of bringing a volatile compound carefully chosen to be deposited onto the surface material. A solid product is formed by one ore more chemical reactions. The non-desired other products must be volatile in order to be removed from the surface. Impurities are avoiding as much as possible, thus the reaction has to be carefully controlled like, for instance, pressure and energy input (*Dépots physiques en phase vapeur*, n.d.). As a matter of fact, CVD technique can be differentiated according to the type of energy used to activate the chemical reaction.

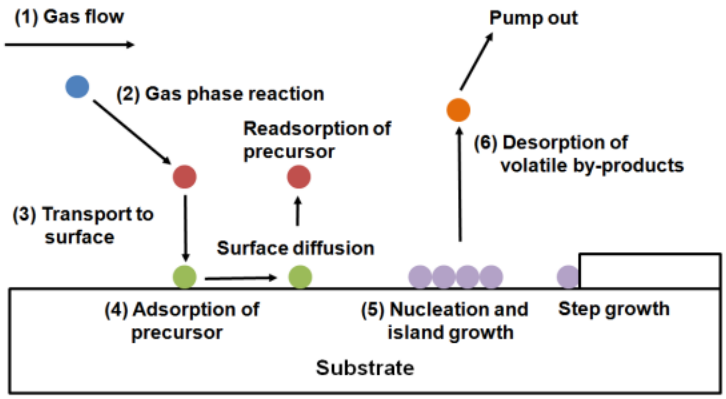

Figure 15: Steps regarding CVD of thin films on a substrate (S. Jeong, 2010)

In that way, this paper puts forward the Metal Organic Chemical Vapor Deposition (MOCVD), showed to be the best, of ZnO (as the steps are displayed in *Figure 15* and *Figure 16*) and Cu_2O (S. Jeong, 2010). For many processes, the final properties of the device depend naturally on several factors. They highlight, for example the type of substrate and precursor, the process pressure and the deposition temperature (S. Jeong, 2010).

In the aim of deposit zinc oxide (ZnO) thin film by CVD, the precursor and the source must contain zinc and oxygen, respectively. The precursor could either be diethyl zinc (DEZ): $Zn(C_5H_5)_2$ or zinc acetylacetonate: $Zn(C_5H_7O_2)_2$, $Zn(acac)_2$ as metal organic compounds.

S. Jeong used a $Zn(C_5H_7O_2)_2$, $Zn(acac)_2$ based precursor instead of a DEZ. Even though DEZ is the most employed precursor due to the facts that the quality film is improved and the easy control of the deposition rate, the manipulation of zinc acetylacetonate is however more accessible.

The CVD set up for ZnO is well defined and described in *Figure 15*. Zinc precursor is located into a steel tank. Some carrier Ar gas is going through in on one side. And on the other side an outlet bonded to the deposition chamber throughout a showerhead. All the lines in red mean that the process is heated in those area thanks to a band heater, and a thermocouple is attached down to the tank in order to regulate the temperature up to 150°C to avoid condensation. A capacitance manometer gauge is connected in between the butterfly and the rotary pump to control the pressure in the range of 1 to 10 Torr. In the end both the precursor and the source, separated in two different flow lines to prevent reaction between these two, are fed into the deposition chamber.

Gases flow rate, such as argon (carrier gas), O_2 as the source and N_2 for venting, are carefully controlled in the range of 0 – 3000 sscm (standard cubic centimetre per minute) by mass flow controller. The substrate is obviously laid on the sample stage heating up to 1000°C according to a resistance heater (S. Jeong, 2010).

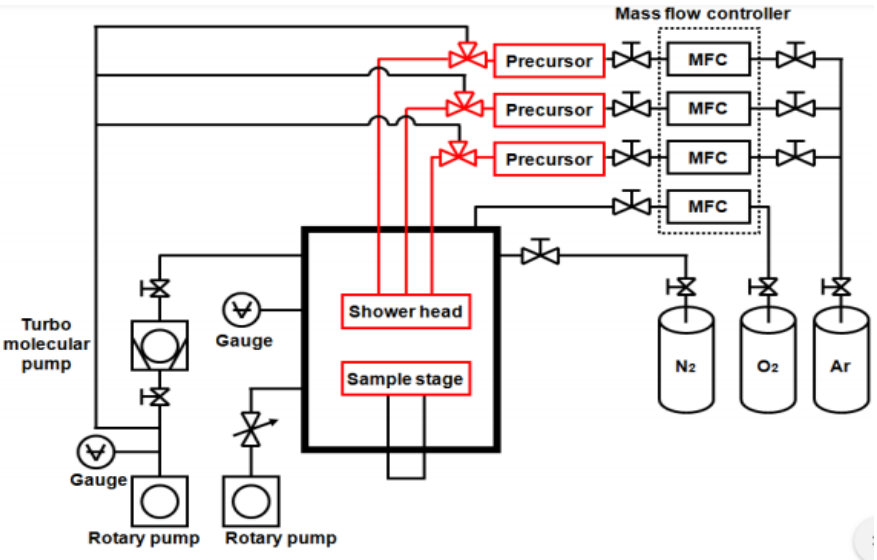

Figure 16: Schematic of ZnO thin film CVD process (S. Jeong, 2010)

As it is going to be put forward in the third section regarding the ZnO/Cu_2O electrodeposition technique, numerous parameters may be modified to reach the best structure and then the best properties of the solar cell device. In this same way, S.Jeong started to show the impact of different parameters regarding the MOCVD process.

First studying the morphology on various substrates. It has been clearly shown that the modification of the substrate to be deposited had a remarkable influence on the ZnO film morphology. To give an example, ss it can be seen in *Figure 16* where X-ray diffraction measurements display that ZnO has a preferential growth direction. In other word, as mentioned in the 2.3.1. part, this is due to its intrinsic properties. Naturally ZnO will tend to grow faster where the formation energy is high, which is for ZnO the normal direction of the plane (c-axis).

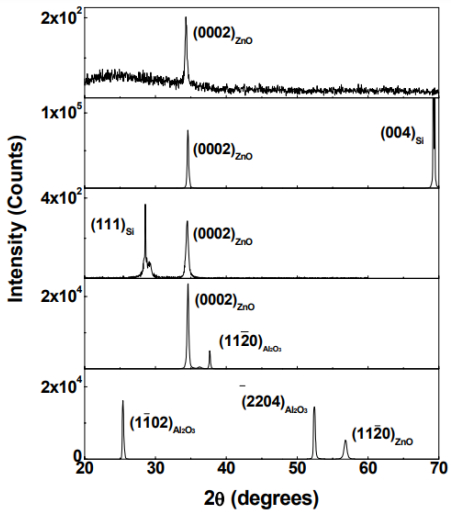

Figure 17: XRD showing morphology dependence on substrates of the growth direction of ZnO : from the top to the bottom (1) Glass ; (2) (100) oriented Si ; (3) (111) oriented Si ; (4) a-plane sapphire ; (5) r-plane spahire (S. Jeong, 2010)

It is also highlighted that the surface may present various morphologies regarding to the temperature deposition of ZnO on r-plane spahire. Mainly the smoothness of the surface is taking into consideration. According to *Figure 18,* which is introduced by Scanning Electron Microscopy (SEM), It is possible to notice the different surfaces behaviour. More the temperature is increasing less the surface tends to be smooth. Higher than 500°C poles growing out appear. Same statement with the Atomic Force Microscope measurements presenting in *Figure 19*. It has been even impossible to measure the surface under 700°C as it was considerably rough.

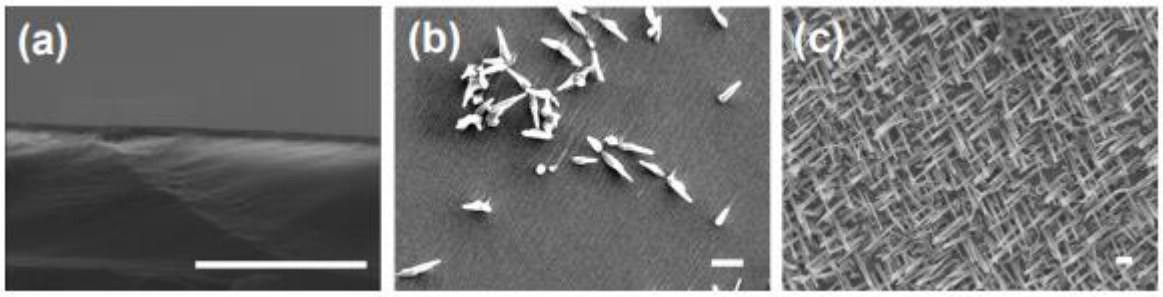

Figure 18: ZnO deposited SEM images (a) 500°C ; (b) 600°C ; (c) 700°C (S. Jeong, 2010)

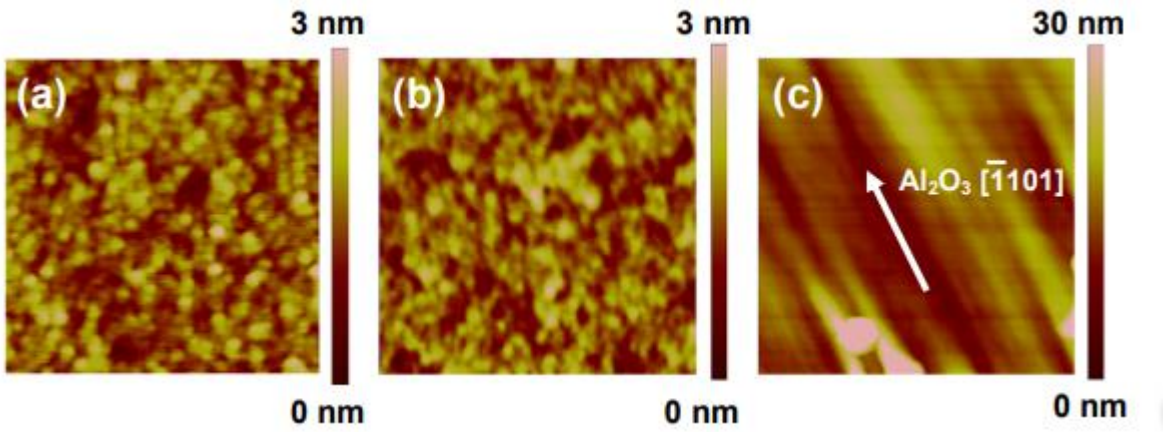

Figure 19: ZnO films deposited AFM images (a) 400°C ; (b) 500°C ; (c) 600°C (S. Jeong, 2010)

That puts up widely the dependence of the deposition parameters that must be highly considered, concerning every types of deposition.

Copper oxide is deposited using MOCVD process as well as shown on *Figure 20* which represents the unfolding of the process. Using a solid hexafluoroactylacetonate cu$(hfac)_2$ powder in a cylindrical tank where the deposited substrate is placed on a heater. To avoid unwanted gas reaction, oxygen and H_2O are fed in the tank through 2 distinct pipes too. Pressure inside the deposition chamber is controlled by butterfly valve.

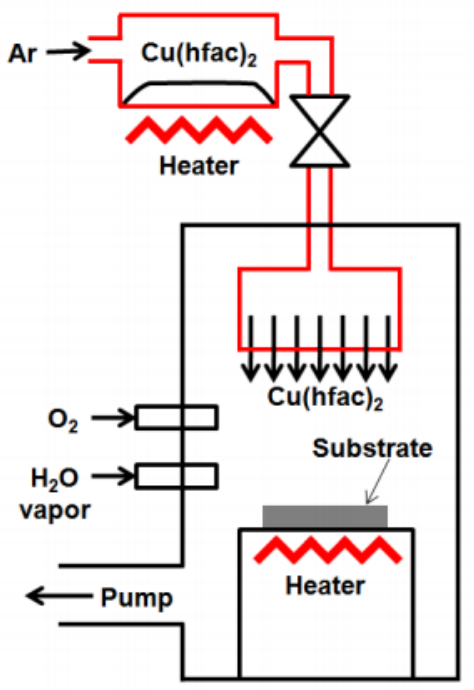

Figure 20: Schematic MOCVD process for Cu_2O deposition (S. Jeong, 2010)

As ZnO, copper oxide shows preferential properties and morpholgy depending on how the substrate surface state is, on which amount of zinc and oxygen there is (Chang & Yeh, 2001), and on what kind of parameters are set during the deposition process, such as the deposition temperature, the thickness… This will be not detailed, because it is not the process used for this subject. It is only to give a preview of the main processes and to give an overview of how Cu_2O/ZnO heterojunction could be upgraded for solar cell regarding the variation of the different deposition parameters. Indeed, it is clearly noticeable that fabrication parameters have a huge influence on the device properties and hence on the efficiency.

The strongest drawback of the CVD is naturally its high cost, which is, here, tried to be as lowest as possible. Beside its benefits other fabrication methods will be preferred, as it will be seen with the electrodeposition method.

It is also comparable to the thermal oxidation method which is going to be explained straight after.

2.4.2. Thermal oxidation

Thermal oxidation is, regarding solar cells, the main manufacturing route used (Siddiqui et al., 2012), so then relevant to talk about. It leads, indeed to high purity structure for semiconductors. However this technique is more appropriate to film and not to this film that is why D. Guo and Y. Ju (Guo & Ju, 2016) investigated ZnO nanowires by thermal oxidation.

First the preparation of ZnO nanowires has been carried out evaporating on the Indium Tin Oxide (ITO) glass substrate a film of zinc under 1 x 10^{-3} Pa at 0,1nm.s^{-1} using electron-beam evaporator. It ended

up with a thickness of about 400 nm. The substrate was undergoing room temperature while zinc film was deposited at 500°C during a day. Nanowires were formed and the cooled down to room temperature.

Afterwards, still using beam-evaporator, copper film was deposited upper the ZnO nanowires under 1 $x10^{-3}$ Pa and at 0,1 $nm.s^{-1}$ to reach a layer thickness of about 500 nm. Everything was deposited at room temperature and at the end heated up to 250°C for one day again to obtain the Cu_2O/ZnO heterojunction.

After characterization, the conclusion was the necessity of tuning growth parameters of Cu_2O layer in order to improve its crystallization to enhance the quality of the p-n junction (Guo & Ju, 2016).

Although thermal oxidation is considering as the best fabrication method for solar cell it still has to be deeply researched in order to reach the best PCE regarding the considered heterojunction.

2.4.3. Electrochemical deposition

The purpose of this section is to present the electrodeposition (or ECD) general method. The fact is that this process is at the heart of our study. Indeed, this deposition method is very versatile, easy to use and therefore very promising for the manufacture of thin-film solar cells. It is known to be potentially expensive in every respect, both economically and energetically. There is no heat treatment, the shape, crystallographic structure, and size of the grains can be modulated, in particular by controlling the pH or adding additives.

Its greatest success is necessarily its very low economic cost, as it does not require any vacuum treatment unlike other processes.

All the parameters that are relevant to the state of the cell and the efficiency will be exposed and explained in the third section dedicated to the “best” manufacture of a Cu_2O/ZnO heterojunction thin fil solar cell.

It does exist a bunch of ECD technique categories. It is possible to cite: electroplating, electrophoretic deposition and underpotential deposition (Hanawa, 2018). Among them, the used technique regarding solar cell is the three-electrode electrochemical cell deposition.

As illustrated in *Figure 21*, the metallic coating is occurred in a conductive bath called electrolyte, which therefore involve ions, both positive and negative. The metal oxide which is going to be deposited must be present in the bath in liquid form dissolved in the water in order to create molten salt. The two principal electrodes are firstly diving into the electrolyte. The one bonded to the positive terminal (anode) is the counter electrode (CE) or the reference electrode and the anode connected to the positive side of the battery is the working electrode (WE). Usually there is a third electrode as known as auxiliary electrode and its responsibility is to carry the current through the cell, on the surface of which no interesting processes take place. The auxiliary electrode provides a circuit to which current is applied or measured. The potential of the auxiliary electrode is usually not measured and is adjusted to balance the reaction occurring at the working electrode. This configuration allows the potential of the working electrode to be measured relative to the known reference electrode without compromising the stability of the reference electrode by passing current through it .

The WE and the CE are basically connected to a power source supply. The movement of the ions in the electrolyte bath is simple, the positively charged ions that are found on the anode are going towards the cathode to link an extra negative charge. The thin layer is thus the deposition of the metallic ions on the cathode. Naturally the nature of the anode, the cathode and the electrolyte bath is carefully chosen based on the experiment led.

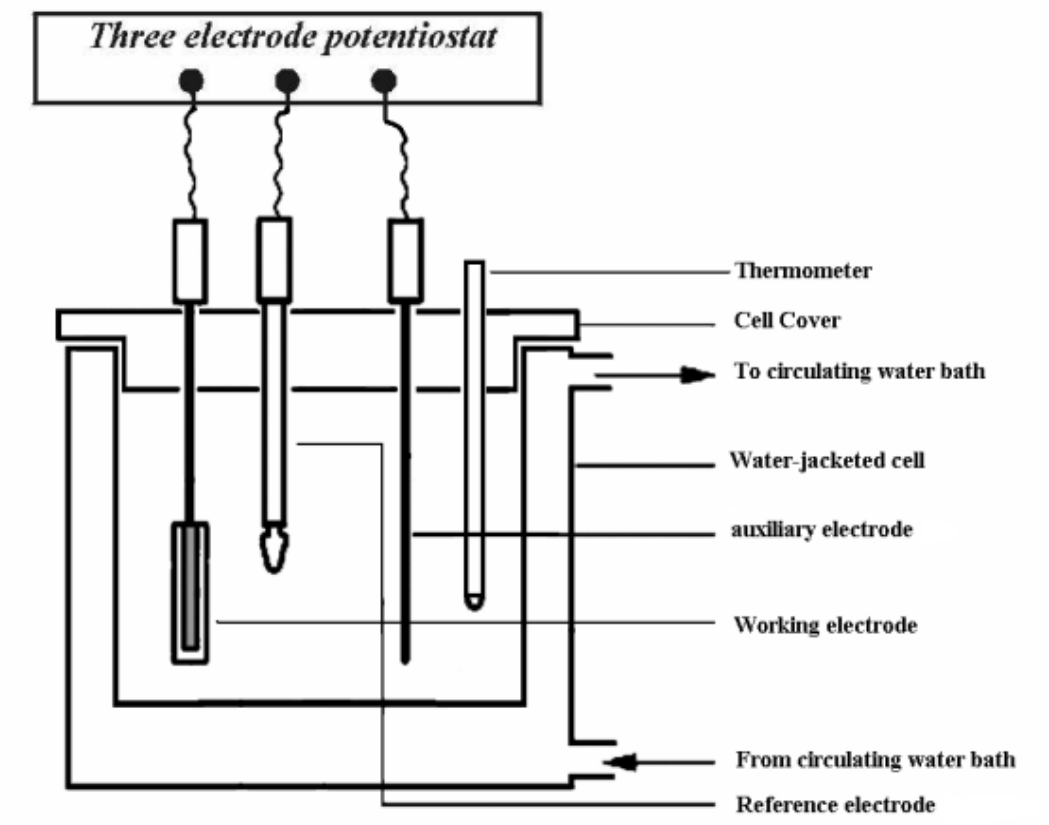

Figure 21: Schematic representation of a three-electrode electrochemical cell (Shahrestani, 2013)

The tremendous things about this technique are that it has low-costs, and it is easy to use. It is therefore very easy to control certain parameters such as thickness with the time duration of the plating and the surface state of our device with the pH and temperature. That will be the state of the other main part in which will be described the influence of this parameters on the cell and then ending up with the best design of the cell choosing the best parameters.

2.5. Methods of characterization

Numerous methods of characterization can be occurred regarding properties of solar cells. They are specific for structural properties and hence for electrical and optical properties. In order to characterize the structure of the cell there is two very know method:

- X-Ray Diffraction (XRD)
- Scanning Electron Microscopy

These two methods will be described below to give a better understanding of how it is working.

2.5.1. X-Ray Diffraction

XRD is a very classical technique for the identification and characterisation of the crystalline structure of materials, which dates to the beginning of the 20th century and has been continuously improved since then. In its ordinary version, used here, it enables the precise measurement of the distances d(hkl) between the different crystal planes (hkl) of a crystal, based on the measurement of the angles of deviation 2θ of an incident X-ray beam (*La Diffraction Des Rayons X | Laboratoire Interfaces et Systèmes Electrochimiques*, n.d.). It enables us to observe the defects and preferred orientation of the thin -film nanostructured crystal. Thanks to the Bragg equation: $2d\sin\theta=n\lambda$ (with λ the wavelength, θ the scattering angle, d the inter-planar distance and n the diffraction order) it gives us the possibility to see the preferable growth direction of the crystal. In fact, crystallites are diffracting X-rays beam with a specific angle to respect Bragg's condition. As schematically explained in *Figure 22* which displays, as already highlighted, that a detector receives X-ray beam from the X-ray source always reflected from the sample with a 2θ angle. Usually when this characterization method is used it is setting out in a graph exhibiting the intensity function of the 2θ angle (Wubet, 2019).

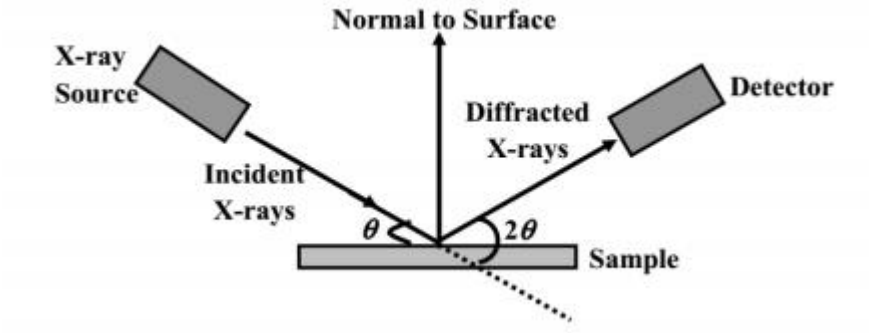

Figure 22: XRD schematic representation (Wubet, 2019)

3.5.2. Scanning Electron Microscopy

The main utilities of the MEB instrument are obviously its given topology, materials composition and morphology information as well as its high-quality three-dimensional image of the studied surface. SEM is scanning a 1 nm circle of the surface sample. The electrons throwing by the source are hitting the sample as showing in the *Figure 23*. Afterwards the topography of the surface is made by the reflection of the generated electrons. Each point in the 1 nm diameter area is scanned to obtain the whole surface representation at each point (Wubet, 2019).

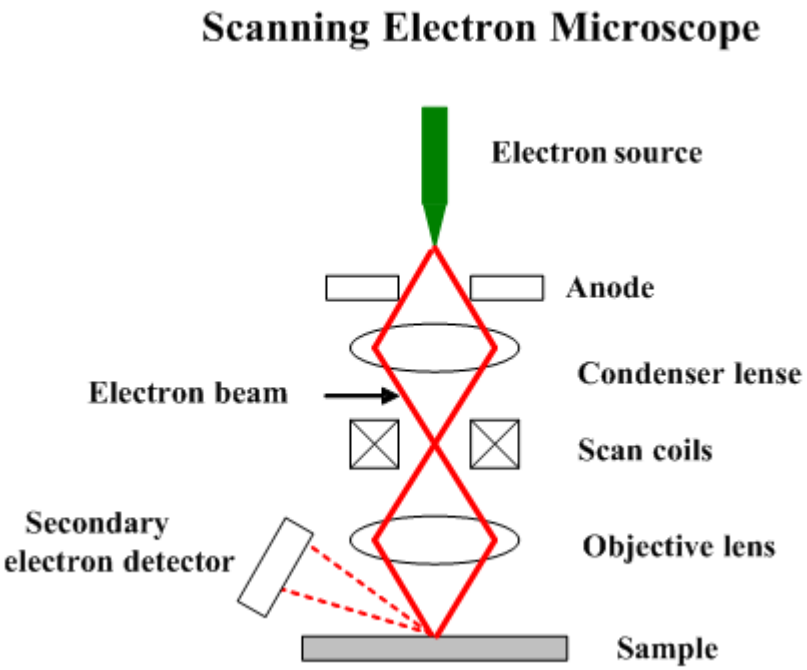

*Figure 23: SEM basic schematic representation method (*Electron_microscope.Png [SubsTech]*, n.d.)*

With the help of these two techniques, it is then conceivable to predict how would be the optical, electrical properties and the efficiency of the device.

2.6. Device efficiency characterization

The surface and the device characterization are likely related to each other. Indeed, if the surface is smooth or exhibit some defects the properties of the cell will not be the same. That is why the surface state is very concerned and mostly the state if the heterojunction surface. Generally, a solar cell is defined by four different main sizes: the External Quantum Efficiency (EQE), the Power Conversion Efficiency (PCE), the open-circuit voltage (V_{OC}) and the short-circuit current (J_{SC}) determined with the current-voltage (J-V) characteristics under illumination (S. Jeong, 2010). This section will, therefore, be dedicated to the presentation of this method.

The electrical power delivered by a photovoltaic cell is the product of the voltage by the current it generates. These two quantities, current and voltage, depend both on the electrical properties of the cell and the electrical load at its terminals. The electrical properties of the cell are synthesised in a graph known as the current-voltage characteristic. Every electric dipole is entirely defined by its current-voltage characteristic, which is unique to it. A random example is given in *Figure 24*.

The point where the J-V curve intersects the tension-axis is called the V_{OC}; this is the voltage at the terminals of the cell when the cell is in open circuit, i.e., when the positive and negative sides are electrically isolated from any other electrical circuit (the current flowing through it is then zero). In this case, the power supplied by the cell ($P = U \times I$) is equal to zero.

The other characteristic point that shows up is the one when the curve hits the current-density axis (y-axis), as well called J_{SC}. Same thing here, this is the current that flows through the photovoltaic cell when it is short-circuited, i.e., when the positive pole is connected to the negative pole (the voltage at its terminals is then zero). In this case, the power supplied by the cell is zero (*GuidEnR PHOTOVOLTAIQUE > Caractéristique Courant-Tension d'une Cellule Photovoltaïque*, n.d.).

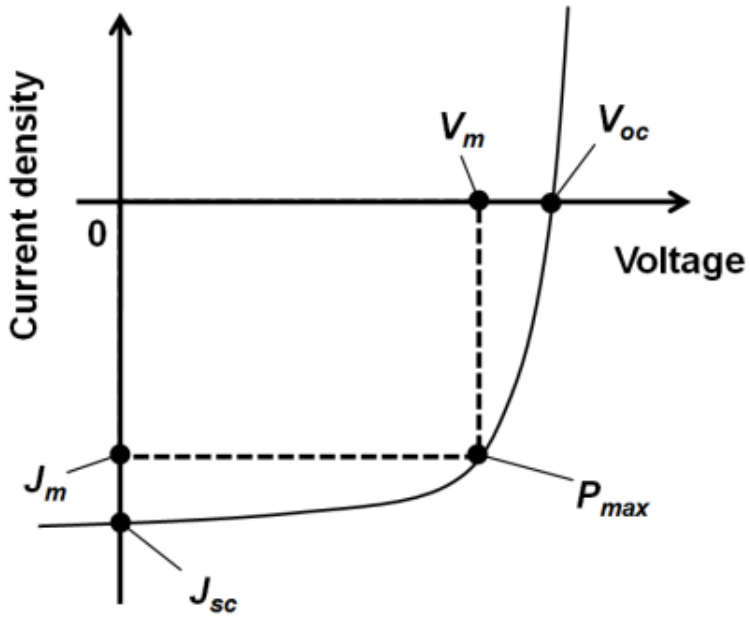

Figure 24: Virtual J-V characteristics illustration for a solar cell under illumination (S. Jeong, 2010)

As illustrated in *Figure 24*, the curve achieves a maximum power, which is important to calculate afterwards the PCE of a solar cell. Knowing that $P_{max} = V_m \times J_m$, it is then possible to get η, the power conversion efficiency of the cell, which is the ratio between P_{max} and P_i (with P_i the illumination power density).

$\eta = \frac{P_{max}}{P_i}$ (S. Jeong, 2010)

PCE and EQE are two similar values to describe the efficiency of the cell but still different. The external quantum efficiency is known to be also the incident-photon-to-current-conversion-efficiency (IPCE).

The spectral response (SR) measurement is elementary to find the EQE of the device. The measure are obtaining thanks to the set up used (Ananda, 2017) in *Figure 25*. EQE is needed to understand the cell behaviour, it is a function of the wavelength given by this formula:

$EQE(\lambda) = \frac{hc}{q\lambda} \; x \; SR$ with λ the wavelength, h Planck's constant, c the light velocity, q the electronic charge, and finally SR corresponds to the ratio of the current that the cell produces and the power that the cell receives (Ananda, 2017).

EQE is then the ratio between the quantity of electrons produced and the total of photons absorbed by the device. In other words, the amount of incident photons that has been converted into electrons, afterwards it is possible to evaluate the recombination rate, which is the main drawback for a solar cell device. As mentioned before this obstacle is partly due to the state of the surface of the deposited semiconductors.

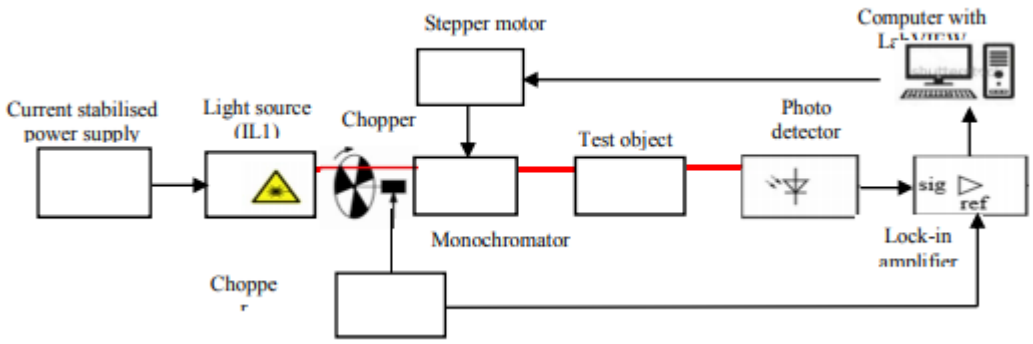

Figure 25: SR measurements set up (Ananda, 2017).

This is naturally where the researche are currently oriented and this will be the topic of this project.

3. State of the project

Thanks to the partnership between my school the Ecole Européenne d'Ingénieurs en Génie des Matériaux (EEIGM) in Nancy and the Universitat Politècnica de València (UPV), I have had the chance to carry out my final master thesis in Spain. Unfortunately, all impacted by the world-known epidemic situation, I never went to the laboratory to lead my experiment on my topic.

As a matter of fact, I decided to turn the experimental part into a proof a concept. The project will then be a gathering of articles that will conduct, for me, to the "best" manufacture of a Cu_2O/ZnO heterojunction thin film solar cell.

In this section, the electrochemical deposition of the copper and the zinc oxide will be exhibited and explained. The variation of different ECD parameters will be highlighted in order to pick the best among them. They will be carefully chosen after studying them with the different characterization methods described in the state of the art.

3.1. Organisation of the work

Firstly, this project began with a bibliographic documentation of the topic presented through the state of the art. The supervisor was kept informed of the progress of the research. A meeting has been organized to give me their insights. After what the non-access to laboratory was still not a fatality. So,

I was waiting for confirmation to have access to it. Finally, after few weeks the access was not granted to me.

I thus installed a simulation software called SCAPS-1D which is used for solar thin-layer simulation. That was my first time using this software. In the end neither my supervisor nor I managed to get results from the software.

Consequently, I settled to give a proof of concept by the articles I read. This will give deeper information of how the structure and the yield of such a cell is influenced by certain parameters during the electrochemical deposition. Hence the design of the cell will be described in the end.

3.2. Parameters influencing the device

3.2.1. Influence of the pH

The control of the bath pH during electroplating is very easy but very important. Indeed, studies show its influence during the deposition of copper oxide, comparing the same ECD device under three different bath treatment. It has been proven firstly, by using XRD, that bath pH changes the preferential growth of the structure of the copper oxide deposited on the zinc oxide. Indeed, at low pH (from 9) the preferential orientation of the crystal is [100] while at pH of 12 and above the [111] orientation of the crystal is favoured. Similarly, for a pH between the two, the [111] structure takes precedence as illustrated in *Figure 26*. On a structural level, the growth of the copper oxide crystal would rather be at pH = 12 which would correspond to the [0001] (S. S. Jeong et al., 2008) oriented structure of zinc oxide. Also shown in *Figure 27*, Cu_2O deposited at pH = 12 display a better morphology with bigger grain and crystals in the form of pyramids of 3 faces, that will increase the minority carrier transport length (Gershon et al., 2012).

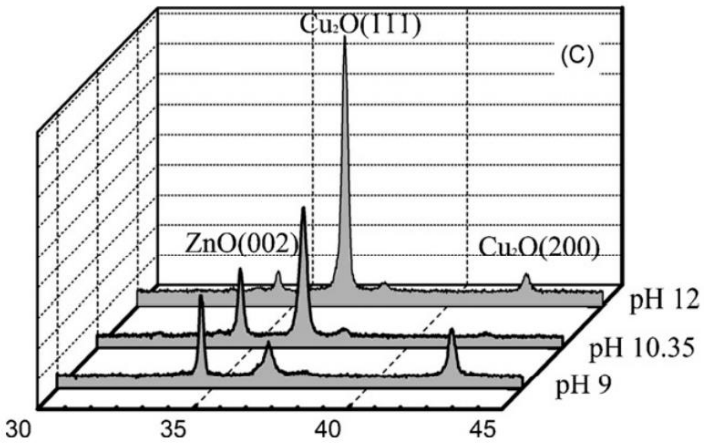

Figure 26: Influence of the pH displaying XRD measurements of three similar heterojunctions (S. S. Jeong et al., 2008).

Beyond the difference in structure, the pH would therefore have an influence on the capacity of the cell. It turns out that the resistivity of the device. The higher the pH, the higher the resistivity. This can be explained by the presence of larger holes when the pH increases (from 10^{12} to 10^{14} cm^{-3}) (S. S. Jeong et al., 2008) and thus increase the photocurrent (Shahrestani, 2013). After all, at pH 12 the displayed cell has the best properties.

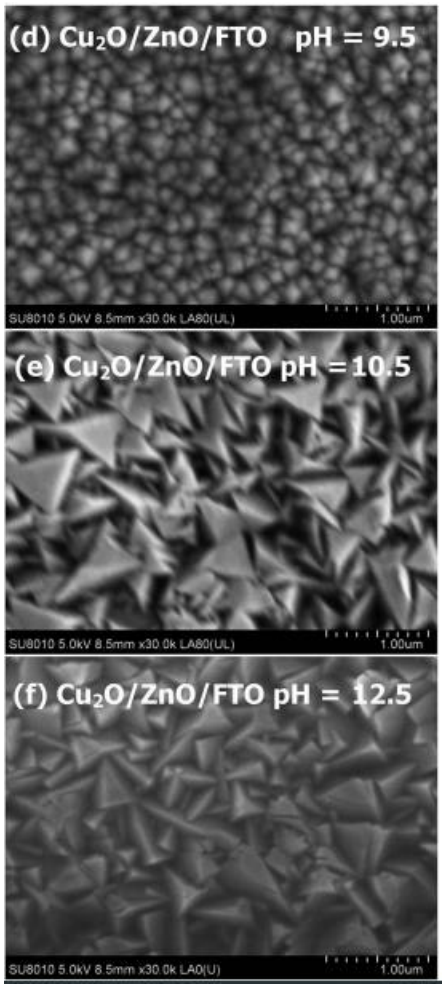

Figure 27: Copper oxide deposited under three different pH bath (d) pH = 9,5 ; (e) pH = 10,5 ; (f) pH = 12,5 (C. Wang et al., 2016)

In the same way, ZnO exhibits preferential structures according to the pH applied during the deposition. As prior revealed, (002) orientation stays the best for thin films regarding transparency. Controlling at the same time other deposition conditions, the pH is investigated as exemplified in *Figure 28*. It is thus easy to conclude that at pH = 2,6 the substrate is completely covered while at higher pH like 4,1 ZnO is under the shape of islets (Illy et al., 2011).

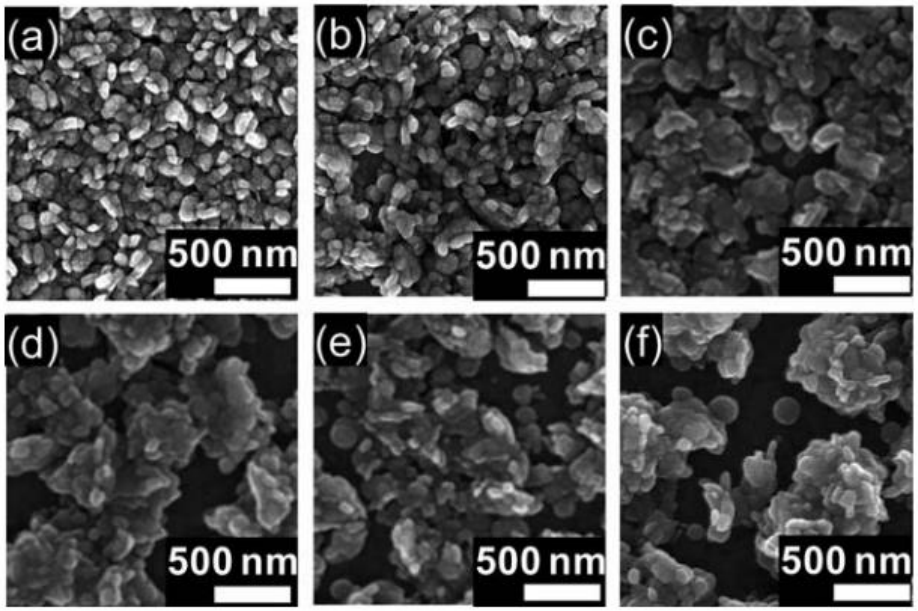

Figure 28: Deposited ZnO under different pH obtained by SEM (a) 2,6 ; (b) 2,9 ; (c) 3,2 ; (d) 3,5 ; (e) 3,8 ; (f) 4,1 (Illy et al., 2011)

3.2.2. Influence of the solution temperature

In addition, it has been put forward that the control of the temperature was crucial. In comparison with the pH, the temperature has also effects on the copper oxide crystalline structure regarding the ECD. At different temperature, cells have been studied through XRD and SEM. Rising the temperature from 40 to 60°C finishes as increasing the intensity of the [111] Cu_2O peak, resulting to an amelioration with crystallinity. However, exceeded 60°C the peak suddenly shrinkage. *Figure 29* shows the images obtained by SEM. It is clearly noticeable that at 40°C the structure put on display small size of grain and textured surface with identifiable defects and voids. At 50°C and 60°C deposition temperature, it is likely to see agglomeration and hence a bigger grains size. Nevertheless, once above 60°C, at 70°C SEM demonstrate pinholes and cracks. The quality or in other words the absorption of the TFSCs is enhanced for an ECD leading at 60°C (Tran et al., 2018).

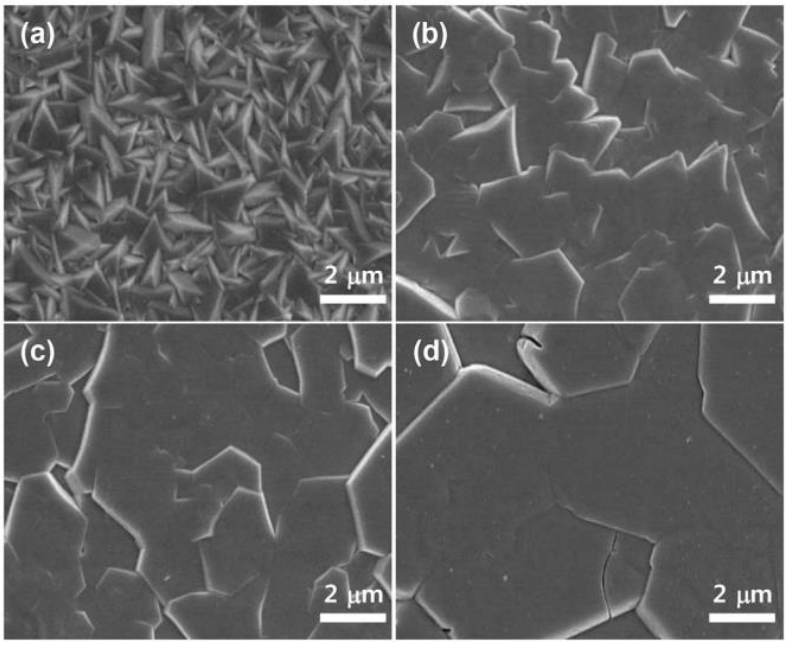

Figure 29: SEM comparison of Cu_2O thin films at various solution temperature (a) 40°C ; (b) 50°C ; (c) 60°C ; (d) 70°C (Tran et al., 2018)

A similar observation can be made with ZnO electrochemical deposition. The preferential growth of the hexagonal structure is facilitated with a temperature bath around 90°C (*Figure 31*). Indeed, between 40 and 50°C plate-like particles are identifiable. At 60°C plate-like particles begin to transform into rod-like particles. The more hexagonal structure occurs at 90°C (Illy et al., 2011).

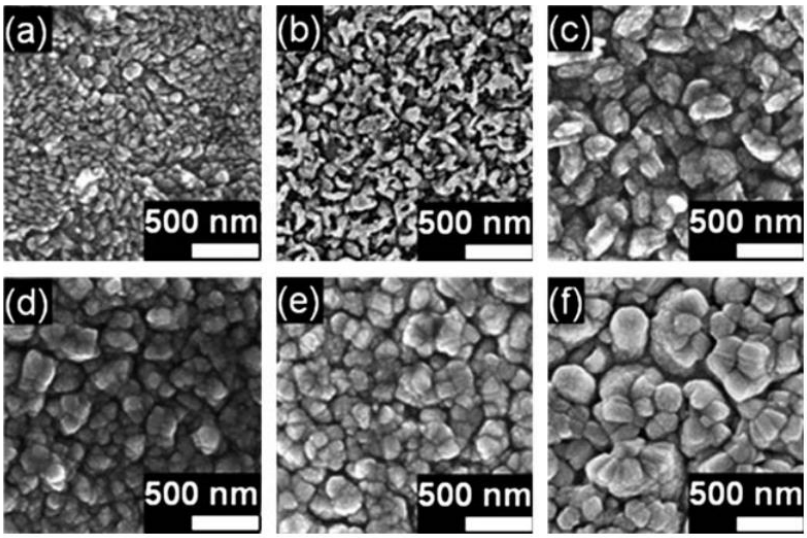

Figure 30: ZnO layer at different temperatures deposition (a) 40°C ; (b) 50°C ; (c) 60°C ; (d) 70°C (e) 80°C (f) 90°C (Illy et al., 2011)

3.2.3. Influence of the thickness

Furthermore, with the negative applied charge, it has been discovered, on the one hand, that the thickness might be change and, on the other hand, that the thickness of both ZnO and Cu_2O layer has a consequential impact on the cell's electrical properties.

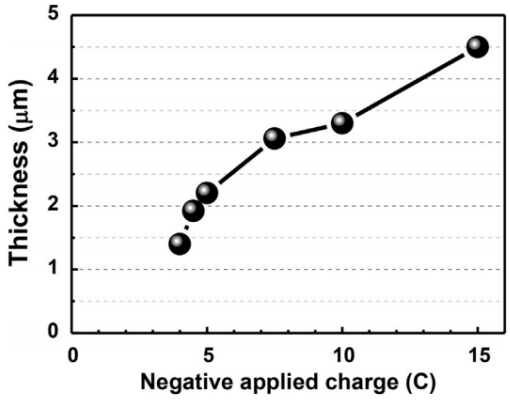

Figure 31: Cu_2O film thickness variation under several negative applied charge (Tran et al., 2018)

The dependence of the thickness with the negative applied charge is shown in *Figure 31*. Three thicknesses were investigated (Tran et al., 2018). The open circuit voltage of the cell demonstrated to increase while the thickness was rising to 3,3 µm but it decreased as soon as the thickness reached up to 4,5 µm. It has been validated that a 3,3 µm copper oxide thin layer displays a better absorption and reduces the physical shunting of such a final cell.

Regarding ZnO ECD, some challenges have been faced. The principal is, undeniably, the thickness controlled once again with the applied voltage. In fact, a thickness less than 300 nm is needed. The V_{oc} of the device increase when the thickness is getting lower.

3.2.4. Influence of the applied potential

The effect of the potential is not negligeable, it is directly related to the thickness of the device and closely linked to the crystalline structure of the two main layers.

It is thus desirable to apply around -430 mV potential in order to keep the copper oxide thickness as close as possible to 3,3 µm and more importantly to increase the single crystalline structure along (111) orientation. Because thanks to XRD measurements (*Figure 32*), it has been proved that this preferential growth direction is more likely to be obtained using -430 mV as potential.

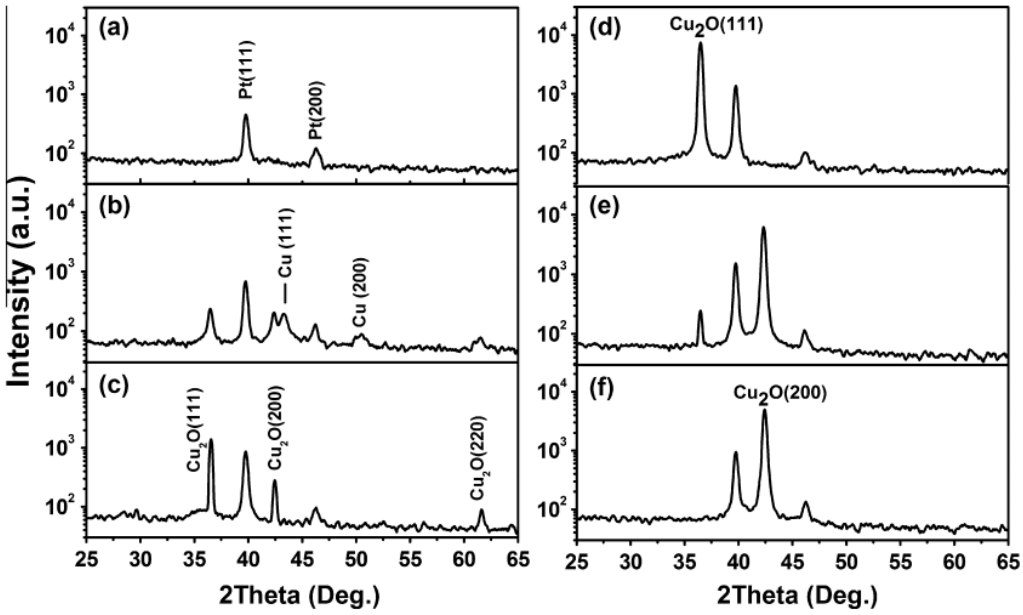

Figure 32: ECD Cu_2O films obtained be XRD under different potential (a) Pt film ; (b) -550 mV ; (c) -520 mV ; (d) -430 mV ; (e) -400 mV ; (f) -340 mV (Elfadill et al., 2015)

By contrast, at -400 and -340 mV applied voltage display a preferred (200) orientation polycrystalline structure which is undesirable.

Same reasoning regarding ZnO. The voltage must keep the preferential thickness while maintaining the formation of the preferential growth. It says that the morphology is not undergoing any change between -1,1 V and -2,0 V whereas individual rods are observed between – 0,8 and -0,9 V. In the range of -1,0 and -1,2 V the nucleation of ZnO is poor and hence the substrate is not fully covered and moreover rods are not growing in the (002) direction. At -1,4 a suspected metallic zinc is formed which is affecting the orientation. A voltage of -1,3 V seems to be the best intermediate.

3.3. Materials and methods

3.3.1. ZnO electrodeposition

A three electrodes deposition has been carried out under very specific condition. The deposited substrate as the WE (the cathode) is an Indium Tin Oxide (ITO) covered glass. ITO is considered as the new generation of solar cells; it has the benefit to be low-priced and flexible and the solar light is easily turned into energy thanks to the various size rods composition of the Transparent Conductive Oxide (TCO). Its carrier concentration is known to be high with impressive electrical conductivity. It also exhibits a great match with the device in order to let zinc oxide growth in its preferential structure orientation. The substrate is first cleaned according to an ultrasonic bath with acetone, methanol, and 0.1 M NaOH solution and deionised water to remove all the surface defaults. Wire of Pt and saturated Ag/Ag chloride played the role of the CE and reference, respectively. Princeton Applied Research potentiostat is useful to monitor the potential and the current.

The concentration of $Zn(NO_3)_2$ introduced in the bath is 130 mM at an applied voltage of -1,3 V under 90°C. The pH of the solution is controlled by adding some acid solution: HCl and fixed at 2,6. Oxygen is removed by bubbling the nitrogen during 20 min and by depositing the copper oxide straight after.

The occurred chemical reaction is: $Zn^{2+} + NO_3^- + 2e^- \rightarrow ZnO + NO_2^-$

3.3.2. Cu_2O electrodeposition

In this case the simple and low-cost ECD occurs with ITO/ZnO as the working electrode using Pt wire as well as counter electrode and silver/silver chloride as reference. The deposition temperature and the pH are kept at 60°C and 12, by carefully adding 4 M of NaOH, respectively. The potential is controlled to be -430 mV during the process. The ECD is prepared by combining 0,2 M of Cu_2O and 3 M of lactic acid. In the end to get the heterojunction as smooth as possible the device is rinsed with water and strengthens at 150°C.

Silver paste is added at the very end to improve the electric conduction regarding the different tests as illustrated in *Figure 33* that shows the final structure of the electrochemically deposited cell.

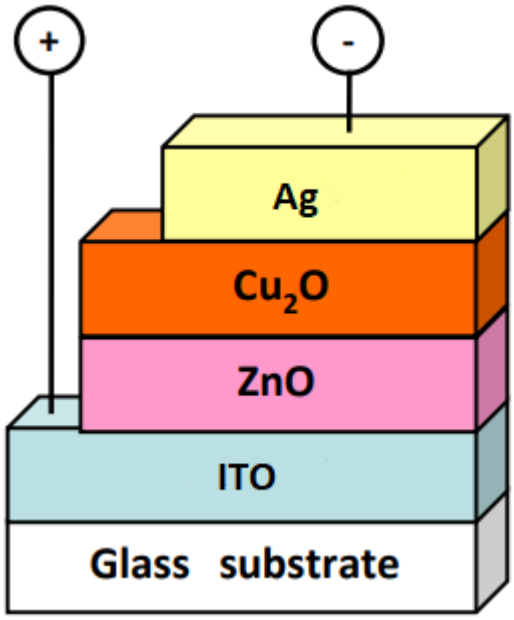

Figure 33: Final design of ZnO/Cu_2O heterojunction solar cell

3.4. Results and discussion

A first series of analysis will be carried out to characterize the different layers constituting the structures. Initially, scanning electron microscopy will be performed on the cross-section of each cell to determine the thickness of the layers. The expected thickness of both ZnO and Cu_2O layer should

be 300 nm and 3,3 µm respectively. X-ray diffractometry will then be used to check the crystallographic structure of the crystalline layers as well as the phase distribution. Diffraction peaks will be displayed in a graph corresponding to each semiconductor layer. As described Cu_2O would show a (111) preferential orientation structure and a raised (002) orientation for ZnO.

Short-circuit current and open-circuit voltage will be exhibited through J-V characteristics using parameters such as 100 $mW.cm^{-2}$ illumination applied by using an AM 1.5 solar simulator. Calculation of the PCE and the EQE will follow to well determine the properties of ZnO/Cu_2O solar cell device.

The PCE might be expected to be around 2% regarding all the deposition parameters, which would be high for this device so far, but still far away of the 20 % PCE that could reach this kind of electrodeposited cell.

4. Conclusion and outlook

The cell has been manufactured combining all the best parameters highlighted so far in the literature. The main factors such as the deposition temperature, the pH, the potential applied, and the thickness have been examined.

Further research should be investigated in order to reduce the defect density, particularly in the Cu_2O layer. The electrons recombination is still too high due to the bad interface at the p-n junction, which prevents the increase of the photo-generated current This could be thus improved by surface etching, thickness, and structural phase control.

Another solution might be adding an organic buffer layer in between zinc oxide and copper oxide. Incorporating a polymer buffer layer could improve the hole injection and blocked the electrons at the surface and thus improved the efficiency. This could be an additional possibility to explore.

References

Abd-Ellah, M., Thomas, J. P., Zhang, L., & Leung, K. T. (2016). Enhancement of solar cell performance of p-Cu2O/n-ZnO-nanotube and nanorod heterojunction devices. *Solar Energy Materials and Solar Cells*, *152*, 87–93. https://doi.org/10.1016/j.solmat.2016.03.022

Ananda, W. (2017). *External quantum efficiency measurement of solar cell* (p. 456). https://doi.org/10.1109/QIR.2017.8168528

Aristidou, N., Eames, C., Sanchez-Molina, I., Bu, X., Kosco, J., Islam, M. S., & Haque, S. A. (2017). Fast oxygen diffusion and iodide defects mediate oxygen-induced degradation of perovskite solar cells. *Nature Communications*, *8*(1), 15218. https://doi.org/10.1038/ncomms15218

Bastos, J. P., Uytterhoeven, G., Qiu, W., Paetzold, U. W., Cheyns, D., Surana, S., Rivas, J., Jaysankar, M., Song, W., Aernouts, T., Poortmans, J., & Gehlhaar, R. (2019). *Model for the Prediction of the Lifetime and Energy Yield of Methyl Ammonium Lead Iodide Perovskite Solar Cells at Elevated Temperatures*. ACS applied materials & interfaces. https://doi.org/10.1021/acsami.9b00923

Benhaliliba, M., Mohra, D., mohamed redha, K., Lahmar, H., Amor, A., & Mourad, M. (2017). *Electrodeposition and Characterization of Cu2O/ZnO/ITO Heterojunction Solar Cell*.

Bergerot, L. (n.d.). *Etude de l'élaboration d'oxyde transparent conducteur de type-p en couches minces pour des applications à l'électronique transparente ou au photovoltaïque*. 232.

Canadian-Solar-Warranty-12-Years.pdf. (n.d.). Retrieved 11 December 2020, from https://www.infiniteenergy.com.au/wp-content/uploads/2019/07/Canadian-Solar-Warranty-12-Years.pdf

Chang, Y., & Yeh, C. (2001). Zinc Oxide/Copper Oxide Mixed Films Deposited by CVD. *MRS Proceedings*, *672*, O8.37. https://doi.org/10.1557/PROC-672-O8.37

Chawake, N. (2014, October 20). Semiconductors: Why ΔE≤3.2 eV ? *Metallurgie Wissen*. https://nirajchawake.wordpress.com/2014/10/20/semiconductors-why-%e2%88%86e%e2%89%a43-2-ev/

Cuprous oxide | metal-powder-dust.com. (n.d.). Retrieved 29 December 2020, from https://www.metal-powder-dust.com/New-Product/cuprous-oxide

Dépots physiques en phase vapeur. (n.d.). ICB-PMDM-LERMPS. Retrieved 3 January 2021, from http://lermps.utbm.fr/activite-et-procedes/depots-en-phase-vapeur/

Domanski, K., Alharbi, E. A., Hagfeldt, A., Grätzel, M., & Tress, W. (2018). Systematic investigation of the impact of operation conditions on the degradation behaviour of perovskite solar cells. *Nature Energy*. https://doi.org/10.1038/s41560-017-0060-5

Eames, C., Frost, J., Barnes, P., O'Regan, B., Walsh, A., & Islam, M. S. (2015). Ionic transport in hybrid lead iodide perovskite solar cells. *Nature Communications*, *6*, 7497. https://doi.org/10.1038/ncomms8497

Electron_microscope.png [SubsTech]. (n.d.). Retrieved 6 January 2021, from https://www.substech.com/dokuwiki/lib/exe/detail.php?id=scanning_electron_microscope&cache=cache&media=electron_microscope.png

Elfadill, N. G., Hashim, M. R., Chahrour, K. M., Qaeed, M. A., & Bououdina, M. (2015). The influence of Cu2O crystal structure on the Cu2O/ZnO heterojunction photovoltaic performance. *Superlattices and Microstructures*, *85*, 908–917. https://doi.org/10.1016/j.spmi.2015.07.010

Fabrication and characterization of copper oxide-zinc oxide solar cells prepared by electrodeposition—IOPscience. (n.d.). Retrieved 5 January 2021, from https://iopscience.iop.org/article/10.1088/1742-6596/433/1/012024

Farooq, A., Hossain, I. M., Moghadamzadeh, S., Schwenzer, J. A., Abzieher, T., Richards, B. S., Klampaftis, E., & Paetzold, U. W. (2018). Spectral Dependence of Degradation under

Ultraviolet Light in Perovskite Solar Cells. *ACS Applied Materials & Interfaces*, *10*(26), 21985–21990. https://doi.org/10.1021/acsami.8b03024

Gershon, T., Musselman, K. P., Marin, A., Friend, R. H., & MacManus-Driscoll, J. L. (2012). Thin-film ZnO/Cu2O solar cells incorporating an organic buffer layer. *Solar Energy Materials and Solar Cells*, *96*, 148–154. https://doi.org/10.1016/j.solmat.2011.09.043

Gibbons, J. F. (1977). *Semiconductor pn junction solar cell and method of manufacture*. Google Patents.

GuidEnR PHOTOVOLTAIQUE > Caractéristique courant-tension d'une cellule photovoltaïque. (n.d.). Retrieved 7 January 2021, from http://www.photovoltaique.guidenr.fr/cours-photovoltaique-autonome-1/caracteristique-courant-tension-cellule-photovoltaique.php

Guo, D., & Ju, Y. (2016). Preparation of Cu2O/ZnO p-n Junction by Thermal Oxidation Method for Solar Cell Application. *Materials Today: Proceedings*, *3*, 350–353. https://doi.org/10.1016/j.matpr.2016.01.019

Hadouchi, W. (2017). *Etude de l'utilisation du ZnO comme contact de type n dans des dispositifs photovoltaïques à base de pérovskite hybride* [Phdthesis, Université Paris Saclay (COmUE)]. https://pastel.archives-ouvertes.fr/tel-01633008

Hamakawa, Y. (2013). *Thin-film solar cells: Next generation photovoltaics and its applications* (Vol. 13). Springer Science & Business Media.

Hamid, H. B. A. (2009). Fabrication, structural and electrical characteristics of zinc oxide (ZnO) thin films by direct current sputtering. *USM Thesis*.

Hanawa, T. (2018). 2.1—Transition of surface modification of titanium for medical and dental use. In F. H. Froes & M. Qian (Eds.), *Titanium in Medical and Dental Applications* (pp. 95–113). Woodhead Publishing. https://doi.org/10.1016/B978-0-12-812456-7.00005-6

Helaili, N. (n.d.). *Synthèse et caractérisation d'oxydes semi-conducteurs basés sur Cu*. 158.

HITACHI. (n.d.). *1. Properties of semiconductors: Hitachi High-Tech GLOBAL*. Retrieved 11 December 2020, from https://www.hitachi-hightech.com/global/products/device/semiconductor/properties.html

IEC 61646—Thin-film terrestrial photovoltaic (PV) modules – Design qualification and type approval | Engineering360. (n.d.). Retrieved 11 December 2020, from https://standards.globalspec.com/std/1093761/IEC%2061646

Illy, B. N., Cruickshank, A. C., Schumann, S., Campo, R. D., Jones, T. S., Heutz, S., McLachlan, M. A., McComb, D. W., Riley, D. J., & Ryan, M. P. (2011). Electrodeposition of ZnO layers for photovoltaic applications: Controlling film thickness and orientation. *Journal of Materials Chemistry*, *21*(34), 12949–12957. https://doi.org/10.1039/C1JM11225B

Işık, T. (2015). *Solar Cells review*. https://doi.org/10.13140/RG.2.1.4298.6404

Jayathilaka, C., Kumara, R., Ohara, K., Song, C., Kohara, S., Sakata, O., Siripala, W., & Jayanetti, S. (2020). Enhancement of Solar Cell Performance of Electrodeposited Ti/n-Cu2O/p-Cu2O/Au Homojunction Solar Cells by Interface and Surface Modification. *Crystals*, *10*, 609. https://doi.org/10.3390/cryst10070609

Jeong, S. (2010). *Thin zinc oxide and cuprous oxide films for photovoltaic applications.* http://conservancy.umn.edu/handle/11299/96486

Jeong, S. S., Mittiga, A., Salza, E., Masci, A., & Passerini, S. (2008). Electrodeposited ZnO/Cu2O heterojunction solar cells. *Electrochimica Acta*, *53*(5), 2226–2231. https://doi.org/10.1016/j.electacta.2007.09.030

Kalogirou, S. A. (2009). Chapter nine—Photovoltaic Systems. In S. A. Kalogirou (Ed.), *Solar Energy Engineering* (pp. 469–519). Academic Press. https://doi.org/10.1016/B978-0-12-374501-9.00009-1

Karam, C. (2017). *ÉLABORATION ET CARACTÉRISATION DES STRUCTURES COEUR-COQUILLE À BASE DE NANOFILS DE ZNO POUR DES APPLICATIONS PHOTOVOLTAIQUES* [Theses, Univ. Montpellier]. https://hal.umontpellier.fr/tel-01681364

Kojima, A., Teshima, K., Shirai, Y., & Miyasaka, T. (2009). Organometal halide perovskites as visible-light sensitizers for photovoltaic cells. *Journal of the American Chemical Society*, *131*(17), 6050–6051. https://doi.org/10.1021/ja809598r

Koussi-Daoud, S. (2016a). *Préparation électrochimique et caractérisation de couches nanostructurées de semi-conducteurs de type p pour cellules photovoltaïques hybrides* [Phdthesis, Université Pierre et Marie Curie - Paris VI]. https://tel.archives-ouvertes.fr/tel-01523449

Koussi-Daoud, S. (2016b). *Préparation électrochimique et caractérisation de couches nanostructurées de semi-conducteurs de type p pour cellules photovoltaïques hybrides* [Phdthesis, Université Pierre et Marie Curie - Paris VI]. https://tel.archives-ouvertes.fr/tel-01523449

La diffraction des rayons X | Laboratoire Interfaces et Systèmes Electrochimiques. (n.d.). Retrieved 5 January 2021, from https://www.lise.upmc.fr/diffractionx

Lee, T. D., & Ebong, A. U. (2017). A review of thin film solar cell technologies and challenges. *Renewable and Sustainable Energy Reviews*, *70*, 1286–1297. https://doi.org/10.1016/j.rser.2016.12.028

Leguy, A. M. A., Hu, Y., Campoy-Quiles, M., Alonso, M. I., Weber, O. J., Azarhoosh, P., Schilfgaarde, M. V., Weller, M. T., Bein, T., Nelson, J., Docampo, P., & Barnes, P. R. F. (2015). Reversible Hydration of CH3NH3PbI3 in Films, Single Crystals, and Solar Cells. *Chemistry of Materials*, *27*(9), 3397–3407. https://doi.org/10.1021/acs.chemmater.5b00660

Luo, Q. (2020). 8—Applications in photovoltaics. In Z. Cui & G. Korotcenkov (Eds.), *Solution Processed Metal Oxide Thin Films for Electronic Applications* (pp. 109–140). Elsevier. https://doi.org/10.1016/B978-0-12-814930-0.00008-6

McEvoy's Handbook of Photovoltaics. (2018). Elsevier. https://doi.org/10.1016/C2015-0-01840-8

Minami, T., Nishi, Y., Miyata, T., & Nomoto, J. (2011). High-Efficiency Oxide Solar Cells with ZnO/Cu2O Heterojunction Fabricated on Thermally Oxidized Cu2O Sheets. *Applied Physics Express*, *4*(6), 062301. https://doi.org/10.1143/APEX.4.062301

Nolan, M., & Elliott, S. D. (2006). The p-type conduction mechanism in Cu2O: A first principles study. *Physical Chemistry Chemical Physics*, *8*(45), 5350–5358. https://doi.org/10.1039/B611969G

NREL. (2019). *Best Research Cell-Efficiencies*. https://www.nrel.gov/pv/assets/pdfs/best-research-cell-efficiencies.20190802.pdf

Olsen, L. C., Addis, F. W., & Miller, W. (1982). Experimental and theoretical studies of Cu2O solar cells. *Solar Cells*, *7*(3), 247–279. https://doi.org/10.1016/0379-6787(82)90050-3

Ozgur, U., Hofstetter, D., & Morkoc, H. (2010). ZnO devices and applications: A review of current status and future prospects. *Proceedings of the IEEE*, *98*(7), 1255–1268.

Resende, J. (2017). *Copper-based p-type semiconducting oxides: From materials to devices*.

Said-Bacar, Z. (n.d.). *Elaboration et caractérisations de silicium polycristallin par cristallisation en phase liquide du silicium amorphe*. 157.

Salek, G. (2013). *Elaboration et caractérisation de films minces absorbants de lumière à partir de dispersions colloïdales de nanoparticules d'oxydes Mn3-xCoxO4(0≤x≤3)et Cu2O* [Phd, Université de Toulouse, Université Toulouse III - Paul Sabatier]. http://thesesups.ups-tlse.fr/2653/

Schwenzer, J., Rakocevic, L., Gehlhaar, R., Abzieher, T., Gharibzadeh, S., Moghadamzadeh, S., Quintilla, A., Richards, B., Lemmer, U., & Paetzold, U. (2018). Temperature Variation Induced Performance Decline of Perovskite Solar Cells. *ACS Applied Materials & Interfaces*, *10*. https://doi.org/10.1021/acsami.8b01033

Shahrestani, S. M. (2013). *Electro deposition of cuprous oxide for thin film solar cell applications*. http://adsabs.harvard.edu/abs/2013PhDT.....606S

Shockley, W., & Queisser, H. J. (1961). Detailed Balance Limit of Efficiency of p-n Junction Solar Cells. *Journal of Applied Physics*, *32*(3), 510–519. https://doi.org/10.1063/1.1736034

Siddiqui, H., Parra, M. R., Pandey, P., Singh, N., Qureshi, M. S., & Haque, F. Z. (2012). A Review: Synthesis, Characterization and Cell Performance of Cu2O Based Material for Solar Cells. *Oriental Journal of Chemistry*, *28*(3), pdf/vol28no3/OJC_Vol28_No3_p_1533-1545.pdf.

Tran, M. H., Cho, J. Y., Sinha, S., Gang, M. G., & Heo, J. (2018). Cu2O/ZnO heterojunction thin-film solar cells: The effect of electrodeposition condition and thickness of Cu2O. *Thin Solid Films*, *661*, 132–136. https://doi.org/10.1016/j.tsf.2018.07.023

Types of Solar Panels: What Are Your Options? | EnergySage. (n.d.). Retrieved 10 December 2020, from https://www.energysage.com/solar/101/types-solar-panels/

Types of solar panels: Which one is the best choice? (n.d.). Solar Reviews. Retrieved 10 December 2020, from https://www.solarreviews.com/blog/pros-and-cons-of-monocrystalline-vs-polycrystalline-solar-panels

Wang, C., Xu, J., Shi, S., Zhang, Y., Liu, Z., Zhang, X., Yin, S., & Li, L. (2016). Structural, optical and photoelectrical properties of Cu2O films electrodeposited at different pH. *RSC Advances*, *6*(6), 4422–4428. https://doi.org/10.1039/C5RA23216C

Wang, T., Yang, X.-Y., Bi, P.-Q., Niu, M.-S., Feng, L., Liu, J.-Q., & Hao, X.-T. (2019). Effective Exciton Dissociation and Reduced Charge Recombination in Thick-Film Organic Solar Cells via Incorporation of Insulating Polypropylene. *Solar RRL*, *3*(8), 1900087. https://doi.org/10.1002/solr.201900087

What are thin film solar panels, how do they work and why aren't they used for residential solar systems? (n.d.). Solar Reviews. Retrieved 10 December 2020, from https://www.solarreviews.com/blog/thin-film-solar-panels

Wubet, W. (2019). *Green Synthesis of CuO Nanoparticles for the Application of Dye Sensitized Solar Cell*.

Yeul, D. M., & Dhote, D. S. (n.d.). *A Review On Applications Of Zinc Oxide Nanostructures*.

Zhou, C., Ghods, A., Yunghans, K., Saravade, V., Patel, P., Jiang, X., Kucukgok, B., Lu, N., & Ferguson, I. (2017). *ZnO for solar cell and thermoelectric applications*. https://doi.org/10.1117/12.2262772

Zinc Oxide Nanoparticles. (n.d.). Indiamart.Com. Retrieved 29 December 2020, from https://www.indiamart.com/proddetail/zinc-oxide-nanoparticles-7956309162.html

5. Estimated Budget

Contents

Index of tables

1. Introduction

This section is an integral part of the TFM presented. It is indeed necessary to give an overview of the budget that a project like this would represent. Naturally, this is an estimated budget and not an exact one. This budget also considers the value added tax (VTA) which represents 21% of the entire budget.

This project must therefore first raise funds and then be explained by the cost description of the materials and machines employed, and the workforce applied.

2. Funding

The funding has been available by the Department of Mechanical and Material Engineering of the Technical and Higher Industrial School of Engineers at the Universitat Politècnica de València (UPV)

3. Budget

3.1 Direct Cost

Regarding the unitary cost of the machine used during this project, the amortization is needed to be calculated following this equation:

$$A = \frac{t \times C}{T}$$

With T considered to be 10 years to amortize the machine, t the machine utilization time to carry out the project, and finally C the real cost of the machine.

Thanks to this equation it has been possible to determine the real device price. Nevertheless, before beginning, it is crucial to say that this budget is totally forecasted because no tests have been made at the laboratory, due to the epidemic situation. However, this part will be a prediction of how much this project could have been cost.

3.1.1. Price of the work force

Table 1: Table of the WF price

Units	Description	Unit price (€)
h	Project Manager	25.00
h	Project co-director	25.00
h	Researcher	25.00
h	Chemical Engineer	18.00
h	Laboratory assistant	15.00

3.1.2. Price of the material

3.1.2.1. Raw materials and components

Table 2: Table of the raw materials and reagents price

Units	Description	Unit price (€)
g	ZnO powder	2.0×10^{-3}
g	Cu_2O powder	8.2×10^{-2}
g	$Zn(NO_3)_2$	2.7×10^{-1}
g	Lactic acid	1.8×10^{-2}
u	HCl	1,6
g	NaOH	2.2×10^{-3}
mL	Solution for Ultrasound	1.179×10^{-2}
mL	Solution of ethanol and acetone	8.7×10^{-4}
u	ITO coated glass 50 mm x 50 mm	16.00

3.1.2.2. Laboratory materials

Table 3: Table of the Laboratory materials price

Units	Description	Unit price (€)
u	Spoon	4.00
u	Beaker 100 mL	1.80
u	Beaker 1 L	9.04
u	Pt wire electrode	44,99
u	Ag/AgCl electrode	130

3.1.2.3. Personal Protective Equipment (PPE)

Table 4: Table of the PPE price

Units	Description	Unit price (€)
u	Latex Gloves	5.2×10^{-2}
u	Extinguisher	26.99
u	Bucket of sand	17.98

Price of the machinery

Table 5: Table of the machinery price

Units	Description	Unit price (€)
h	BRUKER/2D Phaser	4000
h	DA300 - 300mm Dual Beam Scanning Electron Microscope	5320
h	OSSILA Solar I-V test system	2200
h	OSSILA Potentiostat	1770

3.2. Execution budget

Table 6: Executive budget of ZnO/Cu_2O electrodeposition and measurement

Units	Description	Unit price (€)	Quantity	Total (€)
Device fabrication				
h	Chemical engineer	18.00	0.25	4.5
h	Laboratory assistant	15.00	0.25	3.75
g	Cu_2O powder	8.2×10^{-2}	0.2×10^{-4}	$1{,}64 \times 10^{-6}$
g	$Zn(NO_3)_2$	2.7×10^{-1}	0.3×10^{-4}	8.1×10^{-6}
g	Lactic acid	1.8×10^{-2}	0.2×10^{-4}	3.6×10^{-7}
u	HCl	1,6	1	1.6
g	NaOH	2.2×10^{-3}	1	2.2×10^{-3}
mL	Solution for Ultrasound	1.179×10^{-2}	1	1.179×10^{-2}
mL	Solution of ethanol and acetone	8.7×10^{-4}	1	8.7×10^{-4}
u	ITO coated glass 50 mm x 50 mm	16.00	1	16.00
u	Spoon	4.00	1	4.00
u	Beaker 100 mL	1.80	0.2	0.36
u	Beaker 1 L	9.04	0.2	1.808
u	Pt wire electrode	44,99	1	44,99
u	Ag/AgCl electrode	130	1	130

h	OSSILA Solar I-V testsystem	2200	0.30	660
h	OSSILA Potentiostat	1770	0.30	510
			Total price	1377

Table 7: Executive budget of the XRD measurement

Units	Description	Unit price (€)	Quantity	Total (€)
XRD measurement				
h	Chemical engineer	18.00	0.25	4.5
h	Laboratory assistant	15.00	0.25	3.75
h	BRUKER/2D Phaser	4000	0.037	150
			Total price	158,25

Table 8: Executive budget of the XRD observation

Units	Description	Unit price (€)	Quantity	Total (€)
SEM observation				
h	Chemical engineer	18.00	0.25	4.5
h	Laboratory assistant	15.00	0.25	3.75
h	DA300 - 300mm Dual Beam Scanning Electron Microscope	5320	0.037	200
			Total price	208,25

3.2 Overall Budget

Table 9: Overall budget of the research

Description	Price (€)	Quantity	Total (€)
	Executive budget research		
Device fabrication	1377	1	1377
XRD measurement	1208.25	1	158.25
SEM observation	1604.25	1	208.25
		Total price without taxes	1743.5
		10% Overhead costs **10% Know-how**	174.35 174.35
		21% VAT	366.14
		Total Budget	2458,34